AWARD NUMBER: W81XWH-13-1-0211

TITLE: Development of Antidepressants as Novel Agents To Treat Small Cell Lung Cancer

PRINCIPAL INVESTIGATOR: Julien Sage

CONTRACTING ORGANIZATION: Stanford University
Stanford, CA 94305

REPORT DATE: August 2014

TYPE OF REPORT: Annual Report

PREPARED FOR: U.S. Army Medical Research and Materiel Command
Fort Detrick, Maryland 21702-5012

REPORT DOCUMENTATION PAGE

Form Approved
OMB No. 0704-0188

1. REPORT DATE	2. REPORT TYPE	3. DATES COVERED
August 2014	Annual	1 Aug 2013 - 31 Jul 2014

4. TITLE AND SUBTITLE
Development of Antidepressants as Novel Agents To Treat Small Cell Lung Cancer

5a. CONTRACT NUMBER

5b. GRANT NUMBER
W81XWH-13-1-0211

5c. PROGRAM ELEMENT NUMBER

6. AUTHOR(S)
Julien Sage

E-Mail: julsage@stanford.edu

5d. PROJECT NUMBER

5e. TASK NUMBER

5f. WORK UNIT NUMBER

7. PERFORMING ORGANIZATION NAME(S) AND ADDRESS(ES)
Stanford
University,
Stanford CA 94305

8. PERFORMING ORGANIZATION REPORT NUMBER

9. SPONSORING / MONITORING AGENCY NAME(S) AND ADDRESS(ES)
U.S. Army Medical Research and Materiel Command
Fort Detrick, Maryland 21702-5012

10. SPONSOR/MONITOR'S ACRONYM(S)

11. SPONSOR/MONITOR'S REPORT NUMBER(S)

12. DISTRIBUTION / AVAILABILITY STATEMENT
Approved for Public Release; Distribution Unlimited

13. SUPPLEMENTARY NOTES

14. ABSTRACT

Small cell lung cancer (SCLC) is an aggressive neuroendocrine subtype of lung cancer with high mortality. We used a systematic drug repositioning bioinformatics approach querying a large compendium of gene expression profiles to identify candidate U.S. Food and Drug Administration (FDA)-approved drugs to treat SCLC. We found that tricyclic antidepressants and related molecules potently induce apoptosis in both chemonaïve and chemoresistant SCLC cells. The candidate drugs activate stress pathways and induce cell death in SCLC cells, at least in part by disrupting autocrine survival signals involving neurotransmitters and their G protein-coupled receptors. These experiments identify novel targeted strategies that can be rapidly evaluated in patients with neuroendocrine tumors through the repurposing of approved drugs.

15. SUBJECT TERMS
SCLC, small cell lung cancer, tri-cyclic anti-depressants, tricycl

16. SECURITY CLASSIFICATION OF:			17. LIMITATION OF ABSTRACT	18. NUMBER OF PAGES	19a. NAME OF RESPONSIBLE PERSON
a. REPORT	b. ABSTRACT	c. THIS PAGE			USAMRMC
U	U	U	UU	23	19b. TELEPHONE NUMBER *(include area code)*

Table of Contents

Page

INTRODUCTION

The identification of therapeutic approaches for the treatment of cancer is an arduous, costly, and often inefficient process. Drug repositioning, which is the discovery of new indications for existing drugs that are outside their original indications, is an increasingly attractive mode of therapeutic discovery. In addition to saving time and money, an advantageous aspect of drug repositioning is that existing drugs have already been vetted in terms of safety, dosage, and toxicity. Therefore, repurposed candidate drugs can often enter clinical trials much more rapidly than usual. The primary goal of the research funded by this award is to validate candidate drugs identified through a computational repurposing approach against small cell lung cancer and to uncover the mechanisms of action of these drugs.

KEYWORDS

SCLC, small cell lung cancer, drug repositioning, tri-cyclic antidepressants, GPCR signaling

OVERALL PROJECT SUMMARY

Small cell lung carcinoma (SCLC) is a neuroendocrine form of lung cancer. SCLC patients have a 5-year survival of less than 5%. This dismal survival rate has remained the same for the last 30 years and ~200,000 patients die every year worldwide from SCLC, emphasizing the need for the development of novel therapeutic approaches against this aggressive cancer subtype. The idea behind this proposal is to use a drug repositioning approach to identify and validate FDA-approved drugs that can be repurposed to treat SCLC. A unique aspect of our strategy is that we use a novel bioinformatics-based drug-repositioning pipeline based on the analysis of thousands of gene expression profiles experiments.

We had already conducted a preliminary bioinformatics analysis and identified candidate drugs that are predicted to inhibit the growth of SCLC. Among these candidate drugs are inhibitors of G-protein coupled receptors (GPCRs) including anti-depressant molecules; those are novel candidate inhibitors of SCLC. Our objective was to test the effects of these drug candidates on mouse and human SCLC cells in culture and *in vivo* and to identify one or two top candidates, as well as to uncover the mechanisms of action of these candidates. In the past year, we found that tricyclic antidepressants (TCAs) and related molecules potently induce apoptosis in both chemonaïve and chemoresistant SCLC cells. The candidate drugs activate stress pathways and induce cell death in SCLC cells, at least in part by disrupting autocrine survival signals involving neurotransmitters and their G protein-coupled receptors.

Specific tasks and timeline (defined in the initial Statement of Work):

- Task 1 (from now to the beginning of the funding period, including the time required for review and approval processes for mouse studies): expansion and maintenance of the mouse colony to continually generate mice with the appropriate genotypes, including NSG immunocompromised mice. This task has been achieved, but we keep the mouse colony active for new experiments.
- Task 2 (first few months): experiments in mouse and human SCLC and control cell lines to test the effects of the four top candidate drugs. This task has been largely achieved.
- Task 3 (months 1-9): while the first cohorts of mice developing are aging, we will perform short-term experiments in allografts and xenografts transplanted under the skin of NSG mice. The effects of the drugs will be quantified using markers of proliferation, apoptosis, and differentiation. This task has been largely achieved.
- Task 4 (months 6-18): 4-6 months after Ad-Cre infection, tumor development will be measured in *Rb/p53/p130* mutant mice using the luciferase reporter and mice will be treated with the drugs.

Histopathological analysis will be performed, using markers of proliferation and differentiation. This task has been largely achieved.

- Task 5 (months 18-24): we will complete the experiments in Aim 1 in cell lines and mice. This task has been largely largely achieved.
- Task 6 (months 6-12): once we have identified the best cell lines and the top candidate drugs, we will perform the initial experiments to investigate the mechanisms of action of these drugs. In particular, we will measure cell death, cell proliferation, ROS production. This task has been largely achieved.
- Task 7 (months 6-18): we will perform all the experiments for the second part of Aim 2, investigating the role of various GPCRs in promoting survival in SCLC cells. This task has been largely achieved.
- Task 8 (months 18-24): we will use that time to apply for additional funding and to initiate a novel series of experiments (including gene expression profiles, and the analysis of signaling pathways). This task is still in progress.

Please find the data supporting these statements in the manuscript attached (*Cancer Discovery*) [1].

As noted by **Sheila Rowe**, the Science Officer who reviewed the first version of our annual report, we have been more efficient than planned in our timeline and performed a large number of the experiments proposed in the original application just before the grant was awarded. Please note, however, that the grant was awarded August 1st, 2013, and the manuscript was resubmitted 2 weeks later and accepted another week after that, so there is some overalp between the funding time and the final acceptance of the paper, and we have used some of the funds from this award to complete the experiments.

KEY RESEARCH ACCOMPLISHMENTS

- We validated tricyclic antidepressants such as Imipramine as inducers of cell death in SCLC (Aim 1 of the research proposal)
- We determined that TCA treatment inhibit PKA signaling in SCLC cells and leads to increased stress signals eventually resulting in cell death (Aim 2 of the research proposal)

More recent work in the past year (related to the initial Statement of Work):

A number of the initial tasks (presented above) have been largely achieved, but we have been performing a number of related experiments, which are presented below:

1) As discussed in the initial proposal, we have been on the lookout for novel drugs to test. We tested a number of other drugs from the initial drug

Perturbagen_Name	ConnScore	Target/pathway
PHORBOL-12-MYRISTATE-13-ACETATE	-0.3586	PKC (activator)
PHORBOL-MYRISTATE-ACETATE	-0.3496	PKC (activator)
MW-STK33-23	-0.3357	STK33 (inhibitor)
IKK-2-INHIBITOR-V	-0.3252	NfkB (inhibitor)
GSK-2126458	-0.3244	Pi3K (inhibitor)
CCCP	-0.3208	mitochondrial oxidative phosphorylation uncoupler
NCH-51	-0.3164	HDAC (inhibitor)
PURVALANOL-A	-0.3105	CDK (inhibitor)
CGP-71683	-0.3028	NPY (inhibitor)
AS-601245	-0.2997	JNK (inhibitor)
SELAMECTIN	-0.2904	Glutamate-gated Cl receptor (activator)
NNC-55-0396	-0.2883	T-type calcium channel blocker
FCCP	-0.2879	mitochondrial oxidative phosphorylation uncoupler
AG-879	-0.2876	Tyrosine kinase inhibitor (NGFR, VEGFR)
NICLOSAMIDE	-0.2804	mitochondrial oxidative phosphorylation uncoupler
CGK-733	-0.2797	selective inhibitor of ATR and ATM kinases
DOXORUBICIN	-0.2779	Chemotherapeutic
OBATOCLAX	-0.2773	Bcl-2 inhibitor

Figure 1: Computational drug repositioning – top candidate drugs from the second iteration.

repositioning but none of these drugs showed promising results (data not shown). In collaboration with our previous collaborators (Drs. Atul Butte and Purvesh Khatri), we then performed a second drug repositioning analysis *in silico*, using novel gene expression datasets for human SCLC in the literature and improved computational methods. This analysis generated a second list of candidate drugs to test (these candidates are now coined "perturbagens") (see **Figure 1** for the top candidates).

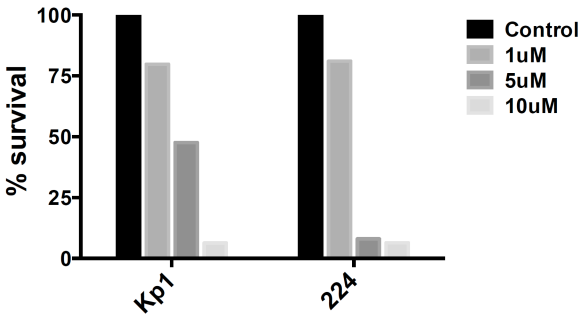

Figure 2: Selamectin induces cell death in mouse SCLC cells in culture (MTT assays) (representative experiments).

Interestingly, we found drugs interacting with signaling pathways that we previously identified as critical in SCLC cells in our *Cancer Discovery* study [1] (e.g. JNK). It is also well known that PI3K [2] and Bcl-2 [3] are playing a role in SCLC cells. We have just begun to validate some of these new compounds and for example wee intrigued by Selamectin, an activator of glutamate-gated chloride channels, which is normally used in pets to kill parasites. Our preliminary observations indicate that this chemical indeed potently induces cell death in SCLC cells in culture (**Figure 2**).

2) At the same time as we are exploring novel candidate drugs, we have continued our analysis of the mechanisms by which TCAs may induce cell death in SCLC cells. In collaboration with the laboratory of Jan Carette at Stanford, we have performed a whole-genome screen [4] to identify genes whose loss-of-function would prevent the induction of cell death by Imipramine; in this screen, every gene in the genome has been disrupted by several retroviral integrations and top candidates are genes for which many independent integrations are shown. The results of this screen are shown in **Figure 3**. Notably, among the top candidates, a number of regulator of cell death were found (e.g. *BCL2L1*, also known as *BCLXL*, or *BAX*, or *PMAIP1* also known as *NOXA*). Very interestingly, *PMAIP1* was initially identified as "Phorbol-12-Myristate-13-Acetate-Induced-Protein-1", which means it is induced by the phorbol ester PMA, itself identified in the new drug repositioning experiment (top hits in Figure 1). We are still trying to understand what these observations are telling us and have begun preliminary experiments to validate these findings.

	Insertions dataset	total dataset	Insertions control	Total control	p-value	p-value corrected for FDR
PMAIP1	106	6667	6	226643	9.90E-155	3.53E-151
BCL2L1	54	6667	24	226643	2.07E-64	3.70E-61
SMARCA4	57	6667	53	226643	2.50E-57	2.97E-54
SLC7A11	40	6667	32	226643	2.25E-42	2.00E-39
BAX	32	6667	13	226643	2.13E-39	1.52E-36
SLC3A2	47	6667	100	226643	1.31E-35	7.79E-33
PBRM1	46	6667	245	226643	9.51E-21	4.85E-18
ATF4	9	6667	2	226643	6.68E-13	2.98E-10
SMARCC1	17	6667	47	226643	2.20E-12	8.72E-10
MED12	7	6667	7	226643	4.49E-08	1.60E-05
BBC3	10	6667	46	226643	3.90E-06	0.001264608
PIBF1	8	6667	40	226643	6.06E-05	0.018010379
ARID1A	6	6667	21	226643	9.63E-05	0.026405852
LOC100129066	14	6667	152	226643	0.000330109	0.084083601
BRD3	5	6667	18	226643	0.00041735	0.097557536
GRRP1	3	6667	3	226643	0.000437723	0.097557536
LUC7L2	7	6667	43	226643	0.000529925	0.105174197
MAX	4	6667	10	226643	0.000530885	0.105174197
TADA3	3	6667	4	226643	0.000749661	0.140699587

Figure 3: Genome-wide haploid genetic screen to identify mediators of cell death by Imipramine in cancer cells. Genes are indicated on the left: red indicates genes that were found in previous creens from the Carette lab and are probably not specific; orange indicates that while the p-value is low, the number of insertions raises some concerns regarding the hit; green indicates the best candidates.

Another interesting candidate from this experiment is *SLC3A2*, which is also known as CD98; it is a solute carrier that can transport amino acids in cells, such as phenylalanine, tyrosine, leucine, arginine and tryptophan. It has been found in a gene fusion event in lung cancer[5] and could play a role in SCLC progression [6]; it may also play a role in metastasis [7]. However, its role in the survival of SCLC cells is completely unknown and we have begun to generate reagents to study its function in SCLC; one

interesting observation is that SLC3A2 interacts with the glucose transporter GLUT1 [8], which raises the possibility that its loss-of-function may affect tumor metabolism.

3) In parallel to these new mechanistic efforts, we have explored the possibility that an alternative mechanism for how TCAs kill neuroendocrine cancer cells: a possible lysosomotropic mechanism in which the drugs may accumulate in lysosomes, blocking their function, thereby leading to cell death. The best known lysosomotropic agent is chloroquine (because its deprotonated form is more membrane-permeable than its protonated form, it is trapped in lysosomes). Our experiments to test this possibility indicate that there may be indeed some induction of cell death in culture in SCLC cells through this mechanism (**Figure 4**), but this is only seen at high doses of the drug (around 20 hours after treatment) and we do not know yet if similar mechanisms may be at play in tumors in vivo.

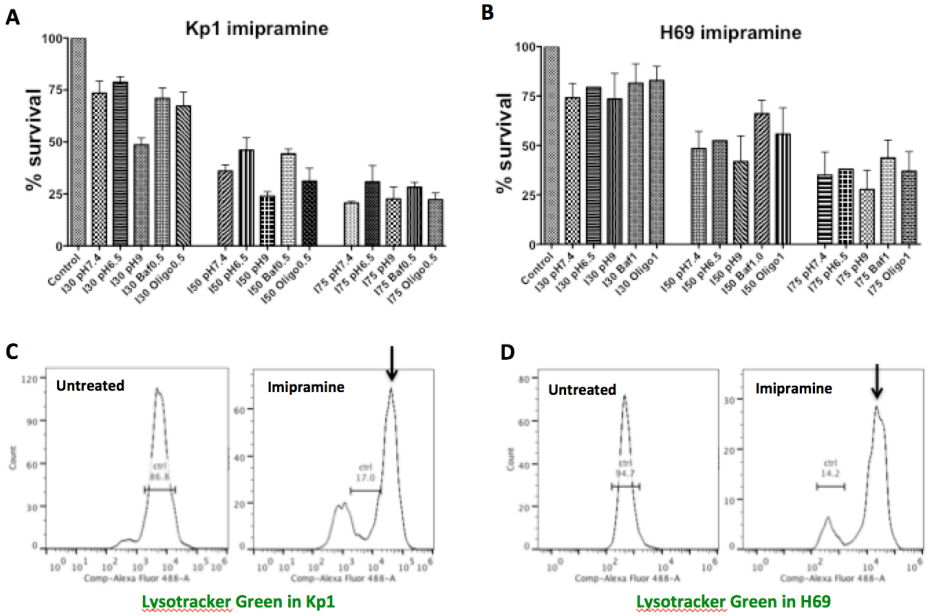

Figure 4: A possible lysosomotropic effect of TCAs in SCLC cells. Kp1 mouse SCLC cells **(A)** and H69 human SCLC cells **(B)** were treated with varying doses of Imipramine at 30 µM (I30), 50 µM (I50), and 75 µM (I75) under different conditions: acidic pH (6.5), alkalinic pH (9), with 0.5 µM or 1 µM of bafilomycin (Baf0.5 or Baf1), and 0.5 µM or 1 µM of oligomycin (Oligo0.5 or Oligo1). Representative FACS histograms of Kp1 **(C)** and H69 **(D)** cells treated with and without 50uM of Imipramine for 20 hours and stained with Lysotracker green. Black arrows depict an increase in Lysotracker signal.

3) Finally, we have been pursuing our analysis of the possible role of PKA downstream of TCAs in SCLC cells: PKA was identified as a key enzyme downstream of TCAs in our previous analysis since PKA activators completely blocked the inhibitory effects of TCAs. This part of the project has been slowed by the long time it has taken to obtain mice in which a point mutation in PKA allows for its specific inactivation using a small molecule inhibitor and at the same time may allow to identify its targets (technology developed by the Shokat lab, [9]). However, to first confirm that PKA is indeed active in SCLC cells, we have used methods developed in the Shokat lab [10-12] to identify active kinases in cells ("inhibitor bead" approach [13]).

Using this platform, we have performed preliminary experiments that have successfully mapped groups of activated kinases in a number of human and mouse SCLC xenografts (Fig. 6). Importantly, among the top candidates identified in these pilot experiment is PKA (**Figure 5**). These experiments solidify our interest in PKA in neuroendocrine tumors.

CONCLUSION

These experiments identify novel targeted strategies that can be rapidly evaluated in patients with neuroendocrine tumors through the repurposing of approved drugs. The goal of the Lung Cancer Research Program is to eradicate deaths from lung cancer to better the health and welfare of the military and the American public. One area of focus for the LCRP is the cure and the control of lung cancer. Our proposal directly addresses this long-term goal because we idnetified novel FDA-approved drugs that can be used to treat patients with SCLC, the most aggressive subtype of lung cancer. Importantly, the smoking rate in the military is still higher than in the rest of the populations (~32% versus ~21%) and SCLC development strongly correlate with cigarette smoking; thus, while the general population may benefit from our work, military personnel may benefit even more from our studies.

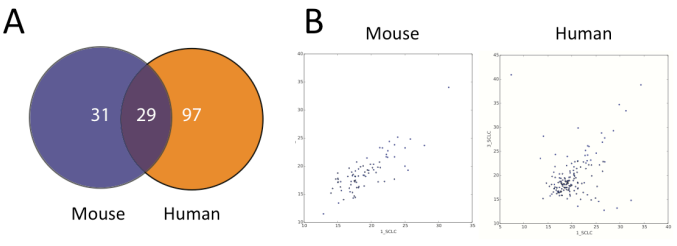

C

	mSCLC vs. Lung		hSCLC vs. NSCLC	
	log2FC	adj.pvalue	log2FC	adj.pvalue
Ephrin type-A receptor 2	-2.99	0	-2.34	0
Tyrosine-protein kinase Lyn	-6.95	0	-0.51	2.77E-03
5'-AMP-activated protein kinase catalytic subunit alpha-1	1.57	0.0005	2.02	0
cAMP-dependent protein kinase catalytic subunit alpha	1.43	1.26E-07	1.21	2.88E-06
Aurora kinase B	6.07	6.11E-14	1.41	2.22E-15
Cyclin-dependent kinase 5	2.82	0	1.58	0
Cyclin-dependent kinase 7	3.20	0	1.59	0
Mitogen-activated protein kinase 9	3.54	0.0082	2.46	0
Mitogen-activated protein kinase 14	2.77	0	1.86	0
Serine/threonine-protein kinase ULK3	1.66	3.94E-07	1.33	2.84E-05

Figure 6. Preliminary inhibitor beads data. A. Schematic of statistically significantly altered kinase to inhibitor beads in mouse SCLC *vs.* mouse lung and human SCLC *vs.* human NSCLC. Relatively lower number of significant kinases in mouse reflects analysis still in process. **B.** Scatter plots of kinase intensity from characteristic pairs of mouse and human SCLC specimens shows greater variability in human specimens. **C**. Table of (preliminaryly) selected shared significantly different kinases between mSCLC and lung and hSCLC and hNSCLC. FC = fold change; p-value adjusted for repeat sampling. PKA is active.

Beyond the publication that has resulted from this work, we have also performed an investigator-driven clinical trial at Stanford (phase 2a, led by Dr. Joel Neal) – this was funded by other funds from the Stanford Cancer Institute. While only a few patients were enrolled, this clinical trial, which is now closed (https://clinicaltrials.gov/ct2/show/NCT01719861?term=NCT01719861&rank=1), was very instructive and will help us initiate a larger trial soon hopefully.

Future/ongoing plans: as discussed above, we have performed a number of "screens" in the past year to refine our drug repositioning analysis but also to better understand the mechanisms underlying our past observations. We will follow up on these screens and top candidates and we will publish the results of the clinical trial. We are also applying for additional sources of funding to pursue this work.

PUBLICATIONS, ABSTRACTS, AND PRESENTATION

a) Publications:

N Jahchan, JT Dudley, PK Mazur, N Flores, D Yang, A Palmerton, AF Zmoos, D Vaka, KQT Tran, M Zhou, K Krasinska, JW Riess, JW Neal, KS Park, P Khatri, AJ Butte*, **J Sage***. A drug repositioning approach identifies tricyclic antidepressants as potent inhibitors of small cell lung cancer and other neuroendocrine tumors. Cancer Discovery, 2013, Dec;3:1364-77. *, co-corresponding authors.

Featured in a New Focus in *Science* (Oct 11, 2013 – "Biology's Dry Future").

Featured in two Perspectives in *Science Translational Medicine* (Oct 16, 2013 – " An anti-depressing discovery for lung cancer treatment" and Oct 30, 2013 – "out with the new, in with the old").

b) Presentations (specifically on this project):

Jan. 2014: invited speaker, Third AACR-IASLC Joint Conference on the Molecular Origins of Lung Cancer, San Diego, CA.

INVENTIONS, PATENTS, AND LICENSES

Nothing to report

REPORTABLE OUTCOMES

As mentioned above, we initiated a clinical trial based on our results.

OTHER ACHIEVEMENTS

Nothing to report

PUBLISHED STUDY

N Jahchan, JT Dudley, PK Mazur, N Flores, D Yang, A Palmerton, AF Zmoos, D Vaka, KQT Tran, M Zhou, K Krasinska, JW Riess, JW Neal, KS Park, P Khatri, AJ Butte*, **J Sage***. A drug repositioning approach identifies tricyclic antidepressants as potent inhibitors of small cell lung cancer and other neuroendocrine tumors. Cancer Discovery, 2013, Dec;3:1364-77. *, co-corresponding authors.

APPENDICES

See publication below.

REFERENCES

1. Jahchan NS, Dudley JT, Mazur PK, Flores N, Yang D, Palmerton A, Zmoos AF, Vaka D, Tran KQ, Zhou M, Krasinska K, Riess JW, Neal JW, Khatri P, Park KS, Butte AJ, Sage J. A Drug Repositioning Approach Identifies Tricyclic Antidepressants as Inhibitors of Small Cell Lung Cancer and Other Neuroendocrine Tumors. Cancer Discov. 2013. PubMed PMID: 24078773. http://www.ncbi.nlm.nih.gov/pubmed/24078773

http://cancerdiscovery.aacrjournals.org/content/early/2013/09/16/2159-8290.CD-13-0183.full.pdf

2. Umemura S, Mimaki S, Makinoshima H, Tada S, Ishii G, Ohmatsu H, Niho S, Yoh K, Matsumoto S, Takahashi A, Morise M, Nakamura Y, Ochiai A, Nagai K, Iwakawa R, Kohno T, Yokota J, Ohe Y, Esumi H, Tsuchihara K, Goto K. Therapeutic Priority of the PI3K/AKT/mTOR Pathway in Small Cell Lung Cancers as Revealed by a Comprehensive Genomic Analysis. J Thorac Oncol. 2014;9(9):1324-31. PubMed PMID: 25122428. http://www.ncbi.nlm.nih.gov/pubmed/25122428

3. Zinn RL, Gardner EE, Dobromilskaya I, Murphy S, Marchionni L, Hann CL, Rudin CM. Combination treatment with ABT-737 and chloroquine in preclinical models of small cell lung cancer. Mol Cancer. 2013;12:16. PubMed PMID: 23452820; PubMed Central PMCID: PMC3599053. http://www.ncbi.nlm.nih.gov/pubmed/23452820

4. Carette JE, Guimaraes CP, Varadarajan M, Park AS, Wuethrich I, Godarova A, Kotecki M, Cochran BH, Spooner E, Ploegh HL, Brummelkamp TR. Haploid genetic screens in human cells identify host factors used by pathogens. Science. 2009;326(5957):1231-5. PubMed PMID: 19965467. http://www.ncbi.nlm.nih.gov/pubmed/19965467

5. Nakaoku T, Tsuta K, Ichikawa H, Shiraishi K, Sakamoto H, Enari M, Furuta K, Shimada Y, Ogiwara H, Watanabe S, Nokihara H, Yasuda K, Hiramoto M, Nammo T, Ishigame T, Schetter AJ, Okayama H, Harris CC, Kim YH, Mishima M, Yokota J, Yoshida T, Kohno T. Druggable oncogene fusions in invasive mucinous lung adenocarcinoma. Clin Cancer Res. 2014;20(12):3087-93. PubMed PMID: 24727320. http://www.ncbi.nlm.nih.gov/pubmed/24727320

6. Kaira K, Ohde Y, Endo M, Nakagawa K, Okumura T, Takahashi T, Murakami H, Tsuya A, Nakamura Y, Naito T, Kondo H, Nakajima T, Yamamoto N. Expression of 4F2hc (CD98) in pulmonary neuroendocrine tumors. Oncol Rep. 2011;26(4):931-7. PubMed PMID: 21750865. http://www.ncbi.nlm.nih.gov/pubmed/21750865

7. Cantor JM, Ginsberg MH. CD98 at the crossroads of adaptive immunity and cancer. J Cell Sci. 2012;125(Pt 6):1373-82. PubMed PMID: 22499670; PubMed Central PMCID: PMC3336374. http://www.ncbi.nlm.nih.gov/pubmed/22499670

8. Ohno H, Nakatsu Y, Sakoda H, Kushiyama A, Ono H, Fujishiro M, Otani Y, Okubo H, Yoneda M, Fukushima T, Tsuchiya Y, Kamata H, Nishimura F, Kurihara H, Katagiri H, Oka Y, Asano T. 4F2hc stabilizes GLUT1 protein and increases glucose transport activity. Am J Physiol Cell Physiol. 2011;300(5):C1047-54. PubMed PMID: 21270293. http://www.ncbi.nlm.nih.gov/pubmed/21270293

9. Morgan DJ, Weisenhaus M, Shum S, Su T, Zheng R, Zhang C, Shokat KM, Hille B, Babcock DF, McKnight GS. Tissue-specific PKA inhibition using a chemical genetic approach and its application to studies on sperm capacitation. Proc Natl Acad Sci U S A. 2008;105(52):20740-5. PubMed PMID: 19074277; PubMed Central PMCID: PMC2634883. http://www.ncbi.nlm.nih.gov/pubmed/19074277

10. Wodicka LM, Ciceri P, Davis MI, Hunt JP, Floyd M, Salerno S, Hua XH, Ford JM, Armstrong RC, Zarrinkar PP, Treiber DK. Activation state-dependent binding of small molecule kinase inhibitors: structural insights from biochemistry. Chem Biol. 2010;17(11):1241-9. PubMed PMID: 21095574. http://www.ncbi.nlm.nih.gov/pubmed/21095574

11. Daub H, Olsen JV, Bairlein M, Gnad F, Oppermann FS, Korner R, Greff Z, Keri G, Stemmann O, Mann M. Kinase-selective enrichment enables quantitative phosphoproteomics of the kinome across the cell cycle. Mol Cell. 2008;31(3):438-48. PubMed PMID: 18691976. http://www.ncbi.nlm.nih.gov/pubmed/18691976

12. Duncan JS, Whittle MC, Nakamura K, Abell AN, Midland AA, Zawistowski JS, Johnson NL, Granger DA, Jordan NV, Darr DB, Usary J, Kuan PF, Smalley DM, Major B, He X, Hoadley KA, Zhou B, Sharpless NE, Perou CM, Kim WY, Gomez SM, Chen X, Jin J, Frye SV, Earp HS, Graves LM, Johnson GL. Dynamic reprogramming of the kinome in response to targeted MEK inhibition in triple-negative breast cancer. Cell. 2012;149(2):307-21. PubMed PMID: 22500798; PubMed Central PMCID: PMC3328787. http://www.ncbi.nlm.nih.gov/pubmed/22500798

13. Sos ML, Levin RS, Gordan JD, Oses-Prieto JA, Webber JT, Salt M, Hann B, Burlingame AL, McCormick F, Bandyopadhyay S, Shokat KM. Oncogene Mimicry as a Mechanism of Primary Resistance to BRAF Inhibitors. Cell reports. 2014;8(4):1037-48. PubMed PMID: 25127139. http://www.ncbi.nlm.nih.gov/pubmed/25127139

Published OnlineFirst September 26, 2013; DOI: 10.1158/2159-8290.CD-13-0183

RESEARCH ARTICLE

A Drug Repositioning Approach Identifies Tricyclic Antidepressants as Inhibitors of Small Cell Lung Cancer and Other Neuroendocrine Tumors

Nadine S. Jahchan[1,2], Joel T. Dudley[1], Pawel K. Mazur[1,2], Natasha Flores[1,2], Dian Yang[1,2], Alec Palmerton[1,2], Anne-Flore Zmoos[1,2], Dedeepya Vaka[1,2], Kim Q.T. Tran[1,2], Margaret Zhou[1,2], Karolina Krasinska[3], Jonathan W. Riess[4], Joel W. Neal[5], Purvesh Khatri[1,2], Kwon S. Park[1,2], Atul J. Butte[1,2], and Julien Sage[1,2]

Published OnlineFirst September 26, 2013; DOI: 10.1158/2159-8290.CD-13-0183

ABSTRACT Small cell lung cancer (SCLC) is an aggressive neuroendocrine subtype of lung cancer with high mortality. We used a systematic drug repositioning bioinformatics approach querying a large compendium of gene expression profiles to identify candidate U.S. Food and Drug Administration (FDA)–approved drugs to treat SCLC. We found that tricyclic antidepressants and related molecules potently induce apoptosis in both chemonaïve and chemoresistant SCLC cells in culture, in mouse and human SCLC tumors transplanted into immunocompromised mice, and in endogenous tumors from a mouse model for human SCLC. The candidate drugs activate stress pathways and induce cell death in SCLC cells, at least in part by disrupting autocrine survival signals involving neurotransmitters and their G protein–coupled receptors. The candidate drugs inhibit the growth of other neuroendocrine tumors, including pancreatic neuroendocrine tumors and Merkel cell carcinoma. These experiments identify novel targeted strategies that can be rapidly evaluated in patients with neuroendocrine tumors through the repurposing of approved drugs.

SIGNIFICANCE: Our work shows the power of bioinformatics-based drug approaches to rapidly repurpose FDA-approved drugs and identifies a novel class of molecules to treat patients with SCLC, a cancer for which no effective novel systemic treatments have been identified in several decades. In addition, our experiments highlight the importance of novel autocrine mechanisms in promoting the growth of neuroendocrine tumor cells. *Cancer Discov; 3(12); 1364–77. ©2013 AACR.*

See related commentary by Wang and Byers, p. 1333.

INTRODUCTION

The identification of therapeutic approaches for the treatment of cancer is an arduous, costly, and often inefficient process. Drug repositioning, which is the discovery of new indications for existing drugs that are outside their original indications, is an increasingly attractive mode of therapeutic discovery. In addition to saving time and money, an advantage of drug repurposing strategies is the fact that existing drugs have already been vetted in terms of safety, dosage, and toxicity. Therefore, repurposed candidate drugs can often enter clinical trials much more rapidly than newly developed drugs (1). Recent advancements in computing, concomitant with the dramatic expansion of available high-throughput datasets, have enabled the development of *in silico* approaches to drug discovery, including the incorporation of genomics-, network-, systems-, and signature-based approaches. Although these computational approaches are still in their infancy, emerging evidence suggests that they enable the discovery of novel treatment options for a wide range of human diseases (2–6).

Lung cancer is the number-one cause of cancer-related deaths in the world, with more than 1.3 million deaths annually. Lung cancer is divided into two major histopathologic groups: non–small cell lung cancer (NSCLC; ~80%–85% of cases) and small cell lung cancer (SCLC; ~15%–20% of cases; refs. 7, 8). SCLC is a very deadly subtype of lung cancer characterized by the rapid expansion and metastasis of small cells with neuroendocrine features. Patients are most commonly diagnosed with metastatic (extensive stage) disease. Without treatment, they may survive only a few weeks to months after the initial diagnosis, but systemic chemotherapy improves the median survival to approach a year. Still, cure is not possible with currently used therapies, and there is no approved targeted therapy for SCLC despite numerous attempts and clinical trials (9). In recent years, a substantial effort from many groups has been made to identify novel treatment options for SCLC. For instance, a proteomic profiling approach has recently identified PARP1 as a novel therapeutic target in SCLC (10). However, it is essential to identify additional therapeutic strategies to block the growth of SCLC tumors.

In this study, we sought to use a systematic drug-repositioning bioinformatics approach to identify novel U.S. Food and Drug Administration (FDA)–approved candidate drugs to treat SCLC. Using this strategy, we identified tricyclic antidepressants (TCA) and related inhibitors of G protein–coupled receptors (GPCR) as potent inducers of cell death in SCLC cells and other neuroendocrine tumors.

RESULTS

To identify novel therapeutic strategies for patients with SCLC, we used a bioinformatics approach that evaluates the

Authors' Affiliations: Departments of [1]Pediatrics, [2]Genetics, and [5]Medicine-Oncology, [3]Vincent Coates Mass Spectrometry Laboratory, Stanford University, Stanford; and [4]Division of Hematology/Oncology, Department of Internal Medicine, University of California Davis Cancer Center, University of California Davis School of Medicine, Sacramento, California

Note: Supplementary data for this article are available at Cancer Discovery Online (http://cancerdiscovery.aacrjournals.org/).

J.T. Dudley and P.K. Mazur contributed equally to this work.

Current address for J.T. Dudley: Department of Genetics and Genomic Sciences, Mount Sinai School of Medicine, New York, NY; current address for P. Khatri: Department of Medicine-Biomedical Informatics Research, Stanford University, Stanford, CA; current address for K.S. Park: Department of Microbiology, University of Virginia, Charlottesville, VA.

Corresponding Authors: Julien Sage, Stanford University, 265 Campus Drive, SIM1 G2078, Stanford, CA 94305-5457. Phone: 650-724-9246; Fax: 650-736-0195; E-mail: julsage@stanford.edu; and Atul J. Butte, Stanford University, 251 Campus Drive West, MSOB X1C63, Stanford, CA 94305-5479. Phone: 650-725-1337; Fax: 650-723-7070; abutte@stanford.edu

doi: 10.1158/2159-8290.CD-13-0183

Published OnlineFirst September 26, 2013; DOI: 10.1158/2159-8290.CD-13-0183

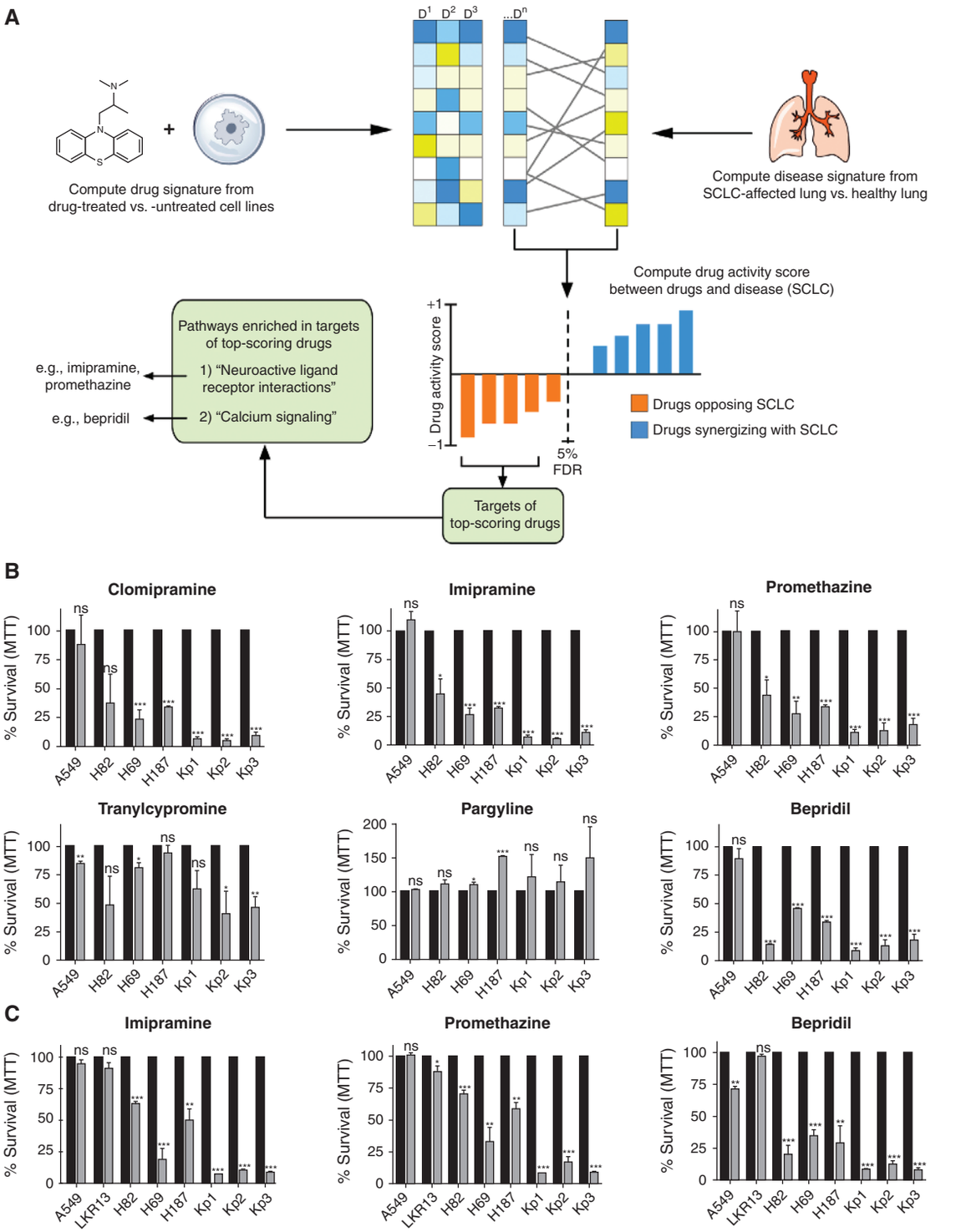

Figure 1. A bioinformatics-based drug-repositioning approach identifies candidate drugs to inhibit SCLC. **A,** schematic representation of the bioinformatics workflow for the repositioning approach used to identify potential candidate drugs for the treatment of SCLC. **B,** representative MTT survival assays of cells cultured in 0.5% serum ($n \geq 3$ independent experiments). A549 are NSCLC cells, H82, H69, and H187 are human SCLC cell lines, and Kp1, Kp2, and Kp3 are mouse SCLC cell lines. Cells were treated for 48 hours with 20 μmol/L clomipramine, 50 μmol/L imipramine, 30 μmol/L promethazine, 100 μmol/L tranylcypromine, 100 μmol/L pargyline, and 10 μmol/L bepridil. **C,** MTT survival assays of NSCLC (A549 and LKR13) and SCLC cells (H82, H69, H187, Kp1, Kp2, and Kp3) cultured in 2% serum ($n > 3$ independent experiments) for 48 hours with 50 μmol/L imipramine, 30 μmol/L promethazine, and 10 μmol/L bepridil. Similar results were obtained in cells growing in dialyzed serum (data not shown). The black bars represent the vehicle-treated cells normalized to 100%. *, $P < 0.05$; **, $P < 0.01$; ***, $P < 0.001$.

Published OnlineFirst September 26, 2013; DOI: 10.1158/2159-8290.CD-13-0183

Table 1. Pathways significantly enriched among top-scoring SCLC-repositioning hits

Pathway name (KEGG ID)	Fold-enrichment	*P*	Gene targets
Neuroactive ligand-receptor interaction (hsa04080)	6.75	1.66×10^{-8}	*GABRA1*, *THRA*, *THRB*, *DRD2*, *GRIN3A*, *ADRA1*, *H1R*, *CHRM5*, *CHRM4*, *HTR1A*, *CHRM3*, *CHRM2*, *CHRM1*, *F2*, *ADRA1B*, *ADRA2A*, *ADRA1A*, *HTR2A*
Calcium signaling pathway (hsa04020)	5.99	3.13×10^{-4}	*CHRM5*, *HRH1*, *CHRM3*, *TNNC1*, *CHRM2*, *CHRM1*, *ADRA1B*, *ADRA1A*, *CACNA1A*, *CALM1*, *HTR2A*
Complement and coagulation cascades (hsa04610)	8.3	1.52×10^{-2}	*F10*, *F2*, *F9*, *F7*, *PROS1*, *PROC*

NOTE: The unique set of canonical targets associated with the top-scoring SCLC-repositioning hits was evaluated for biologic enrichment in KEGG pathways using DAVID. The enrichment statistic *P* values were adjusted for multiple testing using the Benjamini–Hochberg method, and pathways with adjusted $P < 0.05$ are reported as being enriched for targets of top-scoring SCLC-repositioning hits.

therapeutic potential of FDA-approved drugs for a given disease by comparing gene expression profiles in response to these drugs in multiple cell types across multiple diseases (ref. 4; Fig. 1A). From this drug-repositioning approach, we computed a list of candidate drugs with predicted efficacy against SCLC (Supplementary Table S1). This list contained a wide variety of drugs, including some chemotherapeutic agents previously tested with some success in patients with SCLC (e.g., doxorubicin and irinotecan; ref. 7), suggesting that these agents used in the clinic may affect the SCLC gene expression signature. Rather than screen a large number of candidate drugs in cells, we first annotated the known targets of the top-scoring candidates, as well as the pathways enriched in these drug targets (Table 1). This analysis led us to focus on drugs targeting molecules in the "Neuroactive ligand receptor interaction" and "Calcium signaling" pathways, the top two most significant pathways. Notably, SCLC cells are known to express molecules in these pathways, including neurohormonal ligands, channels, and receptors (11–13).

We selected an initial group of six drugs for experimental validation from these two groups. In the "Neuroactive ligand receptor interaction" module, imipramine and clomipramine are two first-generation TCAs with moderate to strong serotonin and epinephrine reuptake inhibition activity, which also display strong anticholinergic, antihistaminic, and antiadrenergic effects. Promethazine is a first-generation histamine H1 receptor antagonist that also possesses anticholinergic and antiadrenergic activities. Tranylcypromine and pargyline are irreversible inhibitors of the enzymes monoamine oxidase A and B, respectively. In the "Calcium signaling pathway," bepridil blocks both voltage- and receptor-operated calcium channels.

We first conducted cell viability assays after exposure to the drugs in culture. As a negative control, we used the lung adenocarcinoma (NSCLC) cell lines A549 (human) and LKR13 (mouse), which are not expected to respond to the same candidate drugs (5). We tested three established human SCLC lines (H82, H69, and H187) and three primary tumor cell lines from a genetically defined mouse model of SCLC (Kp1, Kp2, and Kp3; ref. 14). The doses and concentrations used were optimized for each drug and ranged from 1 to 20 μmol/L for bepridil and 10 to 100 μmol/L for clomipramine, promethazine, imipramine, tranylcypromine, and pargyline; all of these doses have been well documented in multiple cellular contexts. We confirmed that the IC_{50} of these drugs in the human and mouse SCLC cells used was in the same ranges as was previously reported (Supplementary Fig. S1A; data not shown). Next, we used the IC_{80} of the selected drugs to determine the survival of each cell line compared with its vehicle-treated control. Treatment of SCLC cells with imipramine, clomipramine, promethazine, and bepridil, but not tranylcypromine or pargyline, significantly inhibited the growth of mouse and human SCLC cells but not NSCLC cells when cultured in 0.5% or 2% serum (Fig. 1B and C). Cells were also responsive to the drugs in higher serum conditions (5% and 10%; data not shown). Phase contrast images of control and treated SCLC cells suggested that imipramine, promethazine, and bepridil were inducing cell death rather than having cytostatic effects (Supplementary Fig. S1B). Of note, the least responsive SCLC cell line in this initial analysis, H82, is often classified as a variant SCLC cell line with decreased neuroendocrine features.

On the basis of these experiments in culture, we selected one drug in each of the three main categories to carry out experiments *in vivo* (imipramine, promethazine, and bepridil). Once measurable tumors had formed after subcutaneous injection of SCLC cells in immunocompromised NOD.SCID. Gamma (NSG) mice, we treated the transplanted mice for 2 weeks daily with each drug (Fig. 2A). All three drugs inhibited the growth of transplanted mouse Kp1 and Kp3 SCLC cells and human H187 SCLC cells as single agents, although the effects of bepridil were not as significant on the human cell line (Fig. 2B and C and data not shown); promethazine inhibited the growth of human H82 SCLC xenografts significantly, whereas imipramine had a less profound effect (data not shown). We next treated a human primary SCLC tumor growing under the skin of NSG mice with imipramine or promethazine (Fig. 2D) and found that the two drugs had a long-term cytostatic effect on tumor growth (Fig. 2D and E).

These results led us to further investigate the effects and mechanisms of action of the two best candidate drugs, the TCA imipramine and the antihistamine and antiemetic promethazine. To determine the efficacy of the candidate drugs on primary tumors *in vivo*, we examined how endogenous SCLC tumors developing in the lungs of *Rb/p53/p130*–mutant mice (15) responded to drug treatment. Five months after intratracheal instillation of Ad-Cre to delete the three tumor suppressor genes and initiate

Published OnlineFirst September 26, 2013; DOI: 10.1158/2159-8290.CD-13-0183

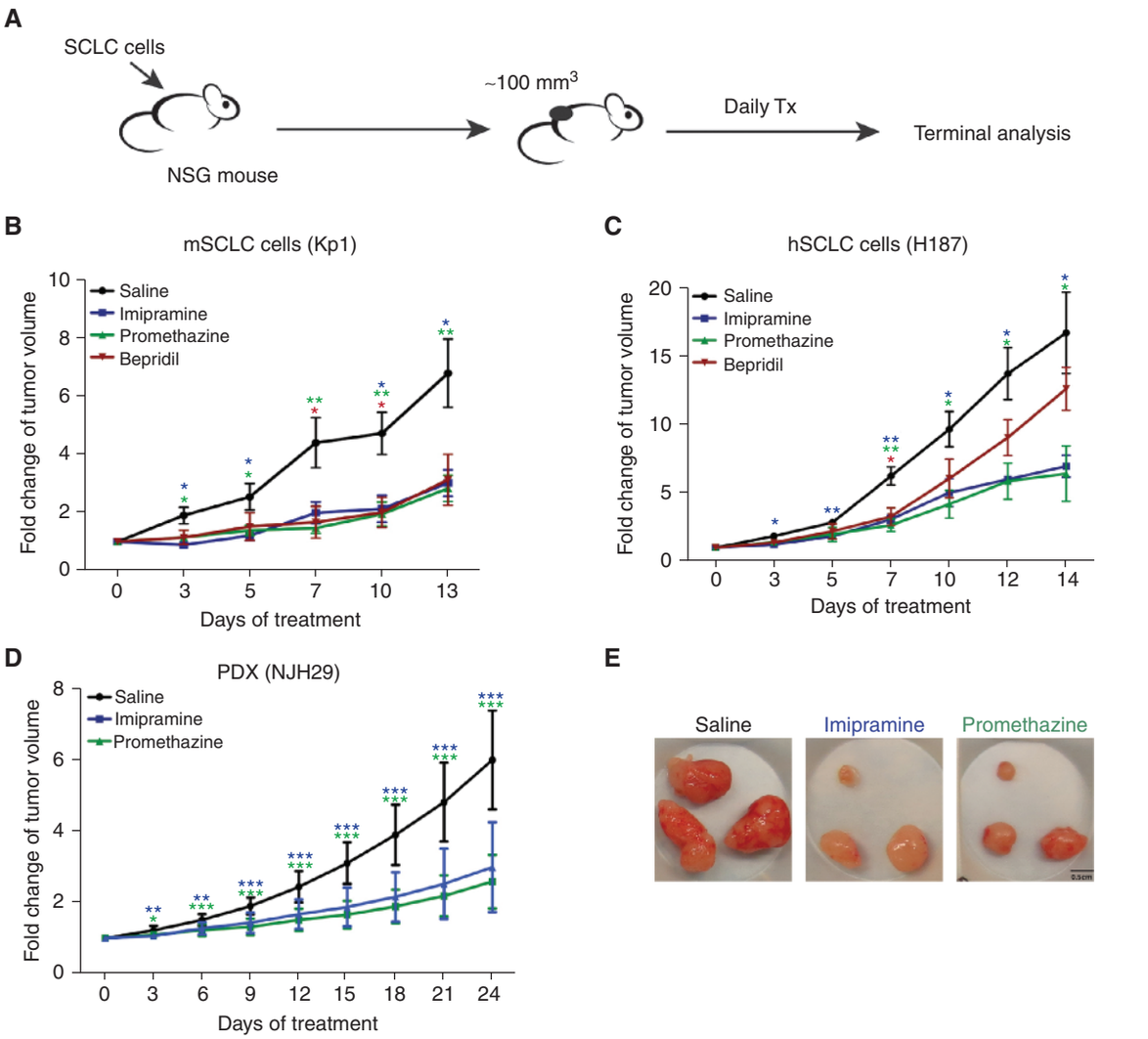

Figure 2. Inhibitory effects of imipramine, promethazine, and bepridil on SCLC allografts and xenografts. **A,** strategy used for the treatment of mice growing SCLC allograft or xenograft tumors under their skin. NSG immunocompromised mice were subcutaneously implanted with one mouse SCLC cell line (Kp1; **B**), one human SCLC cell line (H187; **C**), and one primary patient-derived xenograft (PDX) human SCLC tumor (NJH29; **D**). Tumor volume was measured at the times indicated of daily intraperitoneal injections with vehicle control (saline; $n = 8$ in **B,** $n = 4$ in **C,** and $n = 12$ in **D**), imipramine (25 mg/kg; $n = 5$ in **B,** $n = 4$ in **C,** and $n = 12$ in **D**), promethazine (25 mg/kg; $n = 7$ in **B,** $n = 4$ in **C,** and $n = 9$ in **D**), and bepridil (10 mg/kg; $n = 7$ in **B** and $n = 3$ in **C**; three independent experiments in **B,** one experiment in **C,** and two independent experiments in **D**). Values are shown as the mean ± SEM. An unpaired *t* test was used to calculate the *P* values of imipramine- and promethazine-treated tumors versus saline-treated tumors at different days of treatment. *, $P < 0.05$; **, $P < 0.01$; ***, $P < 0.001$. Values that are not significant are not indicated. **E,** representative images of the primary human SCLC xenografts (NJH29 cells) collected 24 days after daily treatment with saline, imipramine, and promethazine.

tumor development, at a time when these mutant mice have developed advanced lesions, daily intraperitoneal injections of imipramine, promethazine, or saline were carried out on groups of mutant mice. After 30 days of treatment (Fig. 3A), the analysis of whole lungs and hematoxylin and eosin (H&E)–stained sections indicated that imipramine- and promethazine-treated mice had fewer and smaller SCLC tumors than control mice (Fig. 3B). Drug treatment significantly reduced tumor burden as measured by the total tumor area occupying the lungs and the size of the tumors (Fig. 3C and D). Three of 10 control mice developed large metastases in their livers, as described before (15), whereas no large lesions were found in the six promethazine-treated and nine imipramine-treated mice analyzed.

Patients with SCLC are typically treated with a combination of a platinum-based agent and etoposide. Patients often respond well initially but almost invariably relapse with disease that is often resistant to their primary therapy and other agents (9). We observed strong toxicity in tumor-bearing mice simultaneously treated with both cisplatin and etoposide (data not shown), limiting our ability to assess the long-term response of endogenous tumors to both drugs. Consequently, to determine the effects of the candidate drugs on chemoresistant tumors, we treated *Rb/p53/p130;Rosa26*$^{LSL\text{-}Luciferase}$–mutant mice bearing SCLC tumors with saline or cisplatin only, using luciferase expression to monitor tumor burden *in vivo* (Fig. 3E). Tumors that had survived chemotherapy

Published OnlineFirst September 26, 2013; DOI: 10.1158/2159-8290.CD-13-0183

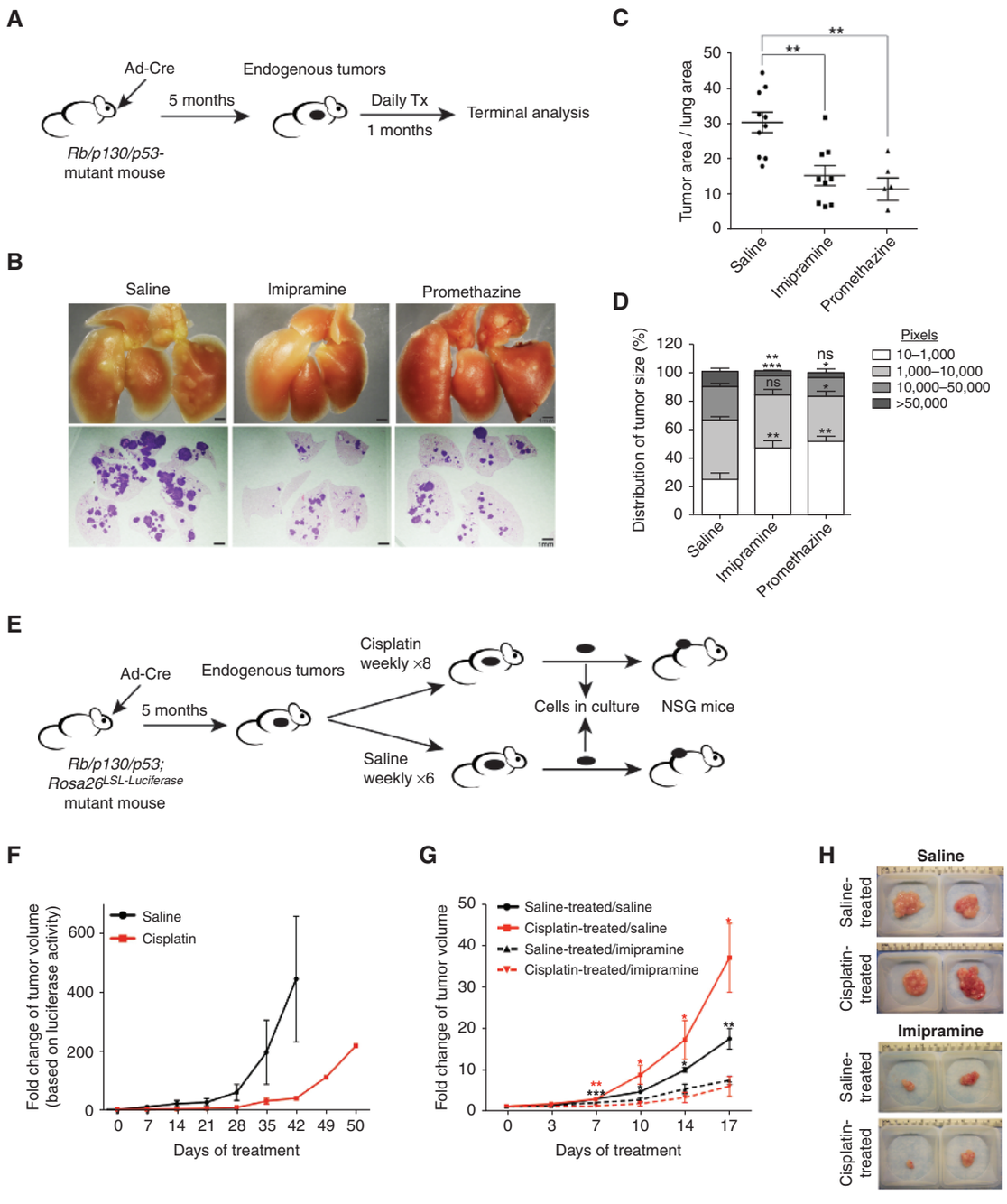

Figure 3. Imipramine and promethazine inhibit the growth of SCLC tumors in a preclinical mouse model. **A,** strategy used for the treatment of *Rb/p53/p130*–mutant mice developing endogenous SCLC tumors. **B,** representative photographs of whole lungs and corresponding H&E-stained sections from mutant mice 6 months after Ad-Cre infection, 1 month after the beginning of treatment with saline, imipramine (25 mg/kg), or promethazine (25 mg/kg). **C,** quantification of the tumor surface area (pixel area units quantified by ImageJ) of mutant mice treated with saline ($n = 10$), imipramine ($n = 9$), and promethazine ($n = 6$; from five independent experiments). An unpaired *t* test was used to calculate the *P* values of imipramine-treated ($P = 0.0017$) and promethazine-treated ($P = 0.0008$) mice compared with control triple knockout mice. **D,** bar graph showing the percentage size distribution of the tumors from mutant mice injected with saline ($n = 10$), imipramine ($n = 9$), and promethazine ($n = 5$). Values are shown as the mean ± SEM. *, $P < 0.05$; **, $P < 0.01$; ***, $P < 0.001$; ns, not significant. **E,** strategy used for the treatment of *Rb/p53/p130;Rosa26*$^{lox\text{-}Stop\text{-}lox\text{-}Luciferase}$ mice developing endogenous SCLC tumors and treated with saline and cisplatin weekly to generate chemonaïve and chemoresistant tumors. Deletion of the *lox-Stop-lox* cassette by Cre allows expression of the reporter and measurement of tumor volume. **F,** fold change of the tumor volume measured by luciferase activity in saline- and cisplatin-treated mice. **G,** NSG mice were subcutaneously implanted with the saline-treated and cisplatin-treated mouse SCLC cells shown in **F** and the fold change of the tumor volume was measured at the times indicated of daily intraperitoneal injections with vehicle control (saline; $n = 4$) and imipramine (25 mg/kg; $n = 4$). Values are shown as the mean ± SEM. An unpaired *t* test was used to calculate the *P* values of imipramine-treated versus saline-treated chemonaïve and chemoresistant tumors at different days of treatment. *, $P < 0.05$; **, $P < 0.01$; and ***, $P < 0.001$. Values that are not significant are not indicated. **H,** representative images of cisplatin- and saline-treated SCLC allografts collected 17 days after daily treatment.

Published OnlineFirst September 26, 2013; DOI: 10.1158/2159-8290.CD-13-0183

and control chemonaïve tumors (Fig. 3F) were then grown in culture or transplanted into immunocompromised recipient mice (Fig. 3E). We found that chemoresistant mouse tumors were inhibited by imipramine treatment similar to chemonaïve tumors both *ex vivo* (data not shown) and in primary allografts (Fig. 3G and H). Thus, tumor cells emerging from long-term treatment with a chemotherapeutic agent are still inhibited by this candidate drug.

Together, these experiments indicate that the expansion of SCLC cells is potently inhibited by imipramine and promethazine and suggest that both chemoresistant tumors and disseminated tumors may respond to treatment in patients with advanced disease.

The visual appearance of SCLC cells treated with imipramine and promethazine in culture suggested that these drugs inhibit SCLC growth by inducing cell death (Supplementary Fig. S1B). Indeed, we found that drug treatment led to apoptotic cell death in culture (data from two representative cell lines, mouse Kp1 cells and human H82 cells), in transplanted tumors, and in endogenous mouse tumors (Fig. 4A–C and Supplementary Fig. S2A and S2B). A concomitant decrease in proliferation was also observed in tumor sections *in vivo* (Supplementary Fig. S2C). Importantly, treatment with the pan-caspase inhibitor zVAD-FMK rescued the cell death induced by imipramine after 24 hours in a dose-dependent manner (Fig. 4D and E), further indicating that apoptotic cell death is a major mechanism by which the candidate drugs inhibit SCLC growth. No induction of cell death was observed in human A549 and mouse LKR13 NSCLC cells in culture at the drug concentrations used (Fig. 1C; Supplementary Fig. S1B; and data not shown) or in the lung epithelium of mice treated daily for 1 month with the candidate drugs, including lung neuroendocrine cells (Supplementary Fig. S2D). We also noted large areas of necrosis in treated tumors (Supplementary Fig. S2B) and found that treatment of SCLC cells with an inhibitor of necrosis also partly rescued the cell death induced by the candidate drugs in culture (Supplementary Fig. S2E). Thus, the candidate drugs induce a rapid cell death specifically in neuroendocrine tumor cells.

Washing out the drugs up to 6 hours after addition to the cells was enough to prevent the appearance of cell death and the decrease in viability observed 24 hours after treatment, whereas exposure of the cells to imipramine for 8 hours or more was sufficient to induce an irreversible cell death in SCLC cells (Supplementary Fig. S3A). This observation allowed us to begin to explore the signaling mechanisms downstream of imipramine treatment in SCLC cells (16, 17). Because the calcium channel blocker bepridil also had some inhibitory effect on SCLC cells (Fig. 1 and Supplementary Fig. S1), we examined changes in calcium levels in response to imipramine and promethazine. We observed a rapid decrease in intracellular calcium levels in SCLC cells after treatment with both drugs (Fig. 4F and Supplementary Fig. S3B and S3C). We also observed increased levels of reactive oxygen species (ROS) after drug treatment (Supplementary Fig. S3D). Increased ROS and oscillations in calcium levels have been directly linked to activation of caspases and apoptotic cell death in certain contexts, including via activation of stress mitogen-activated protein kinase (MAPK) pathways (18). Accordingly, we found changes in the c-*jun*-NH_2-kinase (JNK)/c-Jun pathway upon treatment of SCLC cells with imipramine starting at 1 hour after treatment (Fig. 4G). This rapid activation of the stress MAPK pathway was detected only in SCLC cells and not in mouse or human NSCLC cells (Fig. 4H). Combined treatment of SCLC cells with imipramine and the selective JNK inhibitor SP600125 resulted in a significant rescue of the cell death induced by imipramine (Fig. 4I). Together, these experiments indicate that treatment of SCLC cells with the candidate drugs triggers cellular stresses culminating in apoptotic and necrotic cell death.

The variety of responses triggered by imipramine and promethazine and their known binding to multiple receptors at the surface of cells makes it very likely that one reason they are so effective at inducing death in SCLC is their action on multiple targets. This broad range of action of the candidate drugs may be a positive aspect clinically. Nevertheless, we sought to identify at least some of the molecules targeted by these drugs in SCLC. On the basis of previous pharmacologic studies (19, 20), the dose of imipramine that we used in mice is in the same range as the dose to treat depression in patients, suggesting that the candidate drugs act at least in part through the targets for which they have the highest affinity, including the histamine H1 receptor (H1R), the muscarinic acetylcholine receptor (mAchR; including the CHRM3 isoform), the 5-HT2 serotonin receptor (HTR2; and in particular HTR2a), and the α1-adrenergic receptor (ADRA1a and ADRA1b; refs. 21–26). Our analysis of microarray experiments from human (27–29) and mouse (15) SCLC, binding assays, and previous reports (30–32) indicated that these GPCRs are expressed in SCLC cells (Supplementary Fig. S4A and S4B). These observations led us to treat SCLC cells with related molecules and selective inhibitors of these GPCRs; we also ectopically added purified ligands. Treatment with amitriptyline and desipramine, two first-generation TCAs with high binding affinity to H1R, HTR2, ADRA1, and mAchR; doxazosin mesylate (a selective ADRA1 antagonist); azelastine (H1R); 4-DAMP (CHRM3); and ritanserin (HTR2) in all cases led to a significant reduction in cell survival specifically in SCLC cells and not in NSCLC cells (Fig. 5A and Supplementary Fig. S5A–S5E). Furthermore, the addition of purified epinephrine and of a selective agonist of the H1R to the culture medium was sufficient to increase survival and partially rescued the cell death phenotype induced by promethazine and imipramine (Fig. 5B and Supplementary Fig. S5F). Acetylcholine and serotonin also partially rescued the cell death induced by promethazine, which possesses fewer targets than imipramine (Supplementary Fig. S5G and S5H). Importantly, SCLC cells express the enzymes required for the biosynthesis of the ligands that normally activate the main GPCRs inhibited by this drug (Supplementary Fig. S6A). We also detected the rapid production of serotonin and epinephrine in the supernatant of SCLC cells by mass spectrometry (Supplementary Fig. S6B and S6C). Of note, competition by these endogenous ligands may explain the relatively high concentrations of drugs required to induce cell death in SCLC cells.

Different GPCRs often activate similar downstream signaling pathways, including the $G\alpha_s$ adenyl cyclase/cAMP/protein kinase A (PKA) module and the $G\alpha_q$ phospholipase C β (PLCβ)/protein kinase C (PKC) module (24, 33). Our analysis of microarray experiments indicated that most of

Published OnlineFirst September 26, 2013; DOI: 10.1158/2159-8290.CD-13-0183

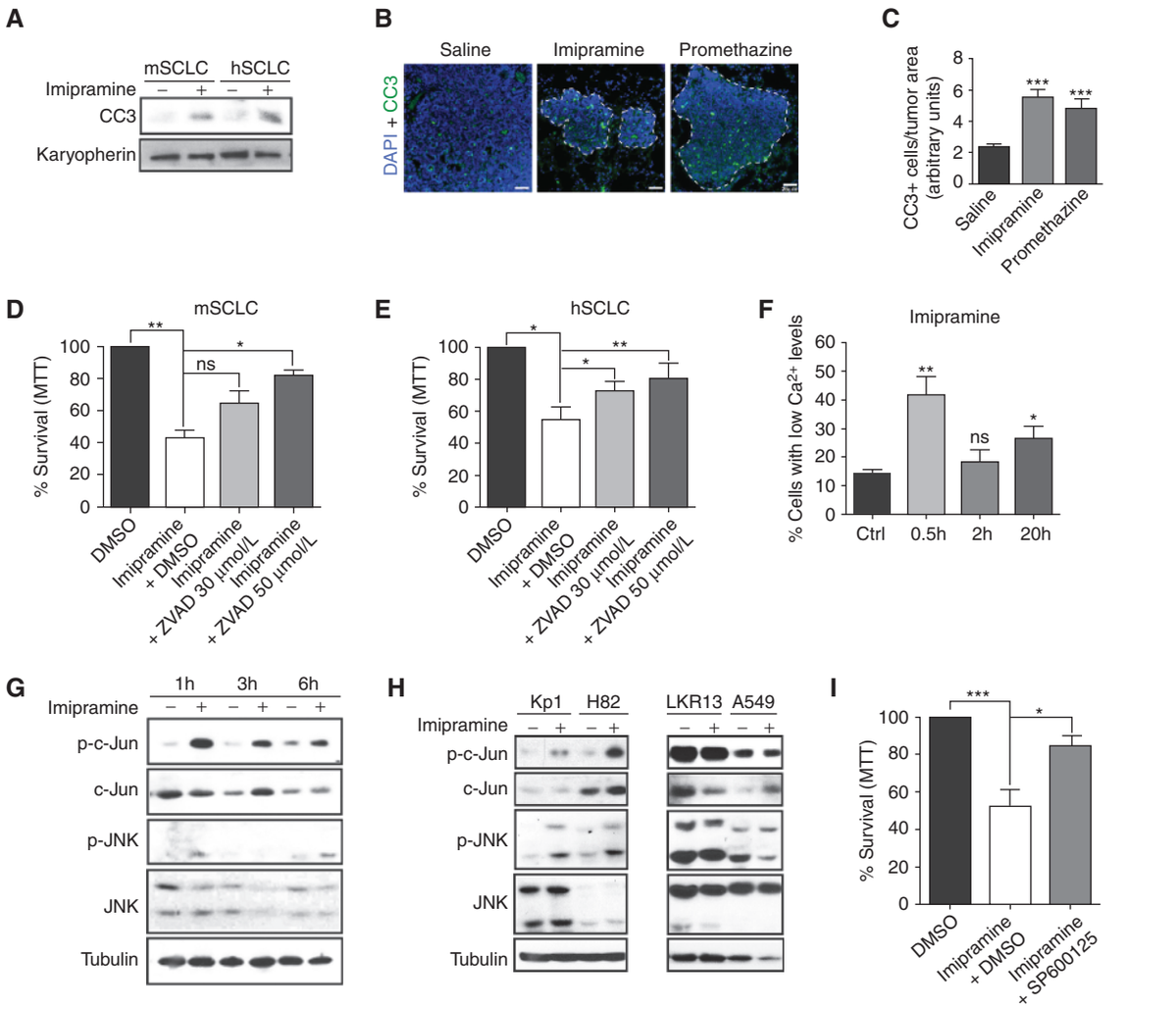

Figure 4. Imipramine and promethazine induce the apoptotic cell death of SCLC cells through activation of caspase-3. **A,** representative immunoblotting of cleaved caspase-3 (CC3) in mSCLC (Kp1) and hSCLC (H82) cells treated with 50 μmol/L imipramine for 12 hours. Karyopherin was used as a loading control. **B,** representative immunostaining of CC3 in tumor sections (white dashed lines) from *Rb/p53/p130*–mutant mice treated daily with saline, imipramine, and promethazine for 30 consecutive days. **C,** quantification of the percentage of CC3-positive cells per tumor area of saline- ($n = 142$ tumors from 10 mice), imipramine- ($n = 153$ tumors from 9 mice; $P < 0.0001$), and promethazine- ($n = 103$ from 6 mice; $P < 0.0001$) treated tumors. **D** and **E,** effects of the combined treatment of imipramine (50 μmol/L) and the pan-caspase inhibitor Z-VAD-FMK on the survival of mSCLC (**D**) and hSCLC (**E**) after 24 hours of treatment, as measured by the MTT viability assay. Values from three independent experiments are shown as the mean ± SEM. The paired *t* test was used to calculate the *P* values of imipramine-treated cells versus control dimethyl sulfoxide (DMSO)-treated cells and of imipramine-treated cells versus Z-VAD-FMK–treated cells combined with imipramine. The black bars represent the vehicle-treated cells normalized to 100%. *, $P < 0.05$; **, $P < 0.01$; ***, $P < 0.001$; ns, not significant. **F,** quantification of the percentage of mSCLC cells (Kp1 and Kp3) with low Ca^{2+} levels by FACS analysis of control untreated cells (Ctrl) and imipramine-treated cells at the times indicated. Values from three independent experiments for each cell line are shown as the mean ± SEM. An unpaired *t* test was used to calculate the *P* values of imipramine-treated cells versus the untreated control cells at the times indicated. *, $P < 0.05$; **, $P < 0.01$; ***, $P < 0.001$; ns, not significant. **G,** representative immunoblotting of p-c-Jun, total c-Jun, p-JNK, and total JNK in mSCLC cells (Kp1) treated with 50 μmol/L imipramine for the indicated times. Tubulin was used as a loading control. **H,** representative immunoblotting of p-c-Jun, total c-Jun, p-JNK, and total JNK in mSCLC cells (Kp1 and H82) and NSCLC cells (LKR13 and A549) treated with 50 μmol/L imipramine for 1 hour. Tubulin was used as a loading control. **I,** effects of the combined treatment of 50 μmol/L imipramine and 500 nmol/L of the JNK inhibitor SP600125 on mSCLC cells (Kp1) after 24 hours of treatment, as measured by the MTT viability assay. Values from three independent experiments are shown as the mean ± SEM. An unpaired *t* test was used to calculate the *P* values of imipramine-treated cells versus control DMSO-treated cells and of imipramine-treated cells versus SP600125-treated cells combined with imipramine. *, $P < 0.05$ and ***, $P < 0.001$. DAPI, 4′,6-diamidino-2-phenylindole.

the different Gα subunits are expressed in SCLC cells, including the $G\alpha_s$ and $G\alpha_q$ subunits (Supplementary Fig. S7A). H1R, CHRM3, ADRA1, and HTR2A are usually thought to be $G\alpha_q$-coupled receptors (26, 34–36), which led us to first test whether blocking PKC signaling may reduce the survival of SCLC cells. However, treatment with the PKC inhibitor GF109203X had no significant inhibitory effect on the survival of mouse and human SCLC cells (Fig. 5C). In addition, treatment with the PKC activator phorbol 12-myristate 13-acetate (PMA) did not rescue the cell death induced by imipramine (Fig. 5D). Accordingly, we did not observe any decrease in phospho-PKC levels (an indicator of PKC activation) at different time points after imipramine treatment in SCLC cells (Fig. 5E and data not shown).

Published OnlineFirst September 26, 2013; DOI: 10.1158/2159-8290.CD-13-0183

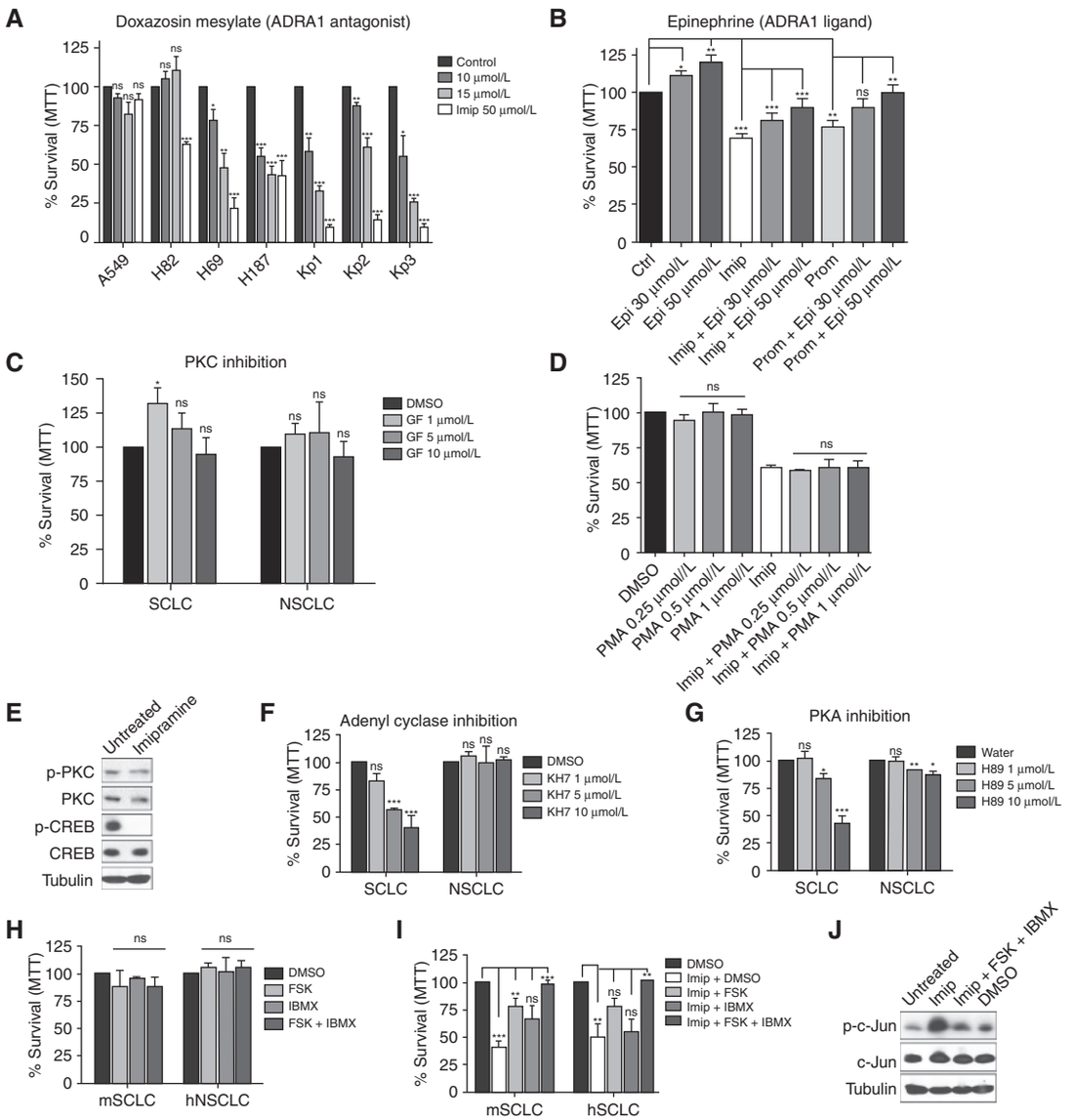

Figure 5. The candidate drugs inhibit the expansion of SCLC cells via several GPCRs. **A** and **B,** MTT viability assays of cells cultured at 2% serum ($n \geq 3$ independent experiments) and treated with the ADRA1 antagonist doxazosin mesylate in comparison with treatment with imipramine (Imip) for 48 hours (**A**) and with increasing doses of epinephrine (Epi) in the absence or presence of 50 μmol/L imipramine or 30 μmol/L promethazine (Prom; **B**). The paired *t* test was used to calculate the *P* values of epinephrine-, imipramine-, and promethazine-treated cells versus control cells and of imipramine- and promethazine-treated cells versus epinephrine-treated cells combined with imipramine or promethazine. *, $P < 0.05$; **, $P < 0.01$; ns, not significant. **C,** MTT viability assay for mSCLC (Kp1) and mNSCLC (LKR13) cells following 48 hours of treatment with increasing doses of the PKC inhibitor GF109203X. Values from three independent experiments are shown as the mean ± SEM. An unpaired *t* test was used to calculate the *P* values of the drug-treated cells versus control cells. *, $P < 0.05$; **, $P < 0.01$; ***, $P < 0.001$; ns, not significant. **D,** MTT viability assay for mSCLC (Kp1) cells following 24 hours of treatment with 50 μmol/L imipramine alone and with increasing doses of PMA in the absence or presence of 50 μmol/L imipramine. An unpaired *t* test was used to calculate the *P* values of dimethyl sulfoxide (DMSO)–treated cells versus PMA-treated cells and of imipramine-treated cells versus PMA-treated cells combined with imipramine. ns, not significant. **E,** representative immunoblotting of p-PKC, total PKC, p-CREB, and total CREB in mSCLC cells (Kp1) untreated and treated with 50 μmol/L imipramine for 30 minutes. Tubulin was used as a loading control. **F** and **G,** MTT viability assay for mSCLC (Kp1) and mNSCLC (LKR13) cells following 48 hours of treatment with increasing doses of the adenyl cyclase inhibitor KH7 (F) and the PKA inhibitor H89 dihydrochloride (**G**). Values from three independent experiments are shown as the mean ± SEM. An unpaired *t* test was used to calculate the *P* values of the drug-treated cells versus control cells. *, $P < 0.05$; **, $P < 0.01$; ***, $P < 0.001$; ns, not significant. **H,** MTT viability assay for mSCLC (Kp1) and hSCLC (H187) cells following 24 hours of treatment with 50 μmol/L forskolin (FSK), 100 μmol/L IBMX, or both drugs combined. An unpaired *t* test was used to calculate the *P* values of the drug-treated cells versus control DMSO-treated cells. ns, not significant. **I,** effects of the combined treatment of 50 μmol/L imipramine and 50 μmol/L FSK alone, 100 μmol/L IBMX alone, or FSK and IBMX together, as measured by the MTT viability assay. Values from at least three independent experiments are shown as the mean ± SEM. An unpaired *t* test was used to calculate the *P* values of imipramine-treated cells versus control DMSO-treated cells and of imipramine-treated cells versus FSK-, IBMX-, and FSK + IBMX–treated cells combined with imipramine. **J,** representative immunoblotting of p-c-Jun and total c-Jun in mSCLC cells (Kp1) untreated, treated with 50 μmol/L imipramine for 30 minutes in the absence or presence of 50 μmol/L forskolin (FSK) and 100 μmol/L IBMX, and treated with DMSO. Tubulin was used as a loading control. The black bars in all the MTT assays represent the vehicle-treated cells normalized to 100%. IBMX, 3-isobutyl-1-methylxanthine.

Published OnlineFirst September 26, 2013; DOI: 10.1158/2159-8290.CD-13-0183

Some reports suggest that, in certain contexts, the GPCRs targeted by the candidate drugs can also signal through $G\alpha_s$ signaling, leading to an increase in adenyl cyclase activity, cAMP levels, PKA activity, and ultimately cAMP-responsive element binding protein (CREB; refs. 37–41). Thus, we next tested the alternative possibility that imipramine and promethazine may induce cell death in SCLC cells by interfering with $G\alpha_s$ signaling. Indeed, we observed a decrease in the phosphorylation of the PKA substrates CREB and activating transcription factor 1 (ATF1) starting at 30 minutes after imipramine treatment in SCLC cells (Fig. 5E and data not shown). To determine the involvement of the $G\alpha_s$ signaling pathway in the survival of SCLC cells and in response to the TCAs, we first treated the cells with inhibitors of this pathway. Treatment with KH7 (an inhibitor of soluble adenyl cyclase) and H-89 dihydrochloride (an inhibitor of PKA) decreased the survival of SCLC cells, but not of NSCLC cells, in a dose-dependent manner (Fig. 5F and G). We next used forskolin and the phosphodiesterase inhibitor 3-isobutyl-1-methylxanthine (IBMX), which are known to activate adenyl cyclase and raised the levels of intracellular cAMP, leading to subsequent PKA activation. Upon addition of forskolin and/or IBMX, alone or in combination, to vehicle-treated mouse and human SCLC cells, no significant increase in cell viability was observed after 24 hours (Fig. 5H). In contrast, the addition of 50 μmol/L of forskolin alone or 100 μmol/L of IBMX alone to imipramine-treated SCLC cells partially rescued the cell death phenotype; full rescue of viability was observed when forskolin and IBMX were added together (Fig. 5I). Finally, the addition of forskolin and IBMX to imipramine-treated cells reverted the elevated levels of phospho-c-Jun to the levels observed in untreated cells (Fig. 5J). These results indicate that imipramine and promethazine induce cell death of SCLC cells by affecting signaling downstream of the $G\alpha_s$ subunit of the targeted GPCRs, thereby inhibiting the adenyl cyclase and cAMP-dependent activation of PKA and inducing cell death via activation of the JNK/c-Jun module (42).

Although the candidate drugs probably bind to multiple targets in SCLC cells, these experiments suggest that the potent effects of these drugs in the induction of cell death in SCLC cell populations are mediated at least in part by the capacity of these drugs to disrupt autocrine survival loops between neurotransmitters and their receptors at the surface of SCLC cells. These observations in SCLC led us to hypothesize that other neuroendocrine tumors may have similar signaling networks as SCLC cells and may be sensitive to the same drugs. The analysis of the few publicly available microarray experiments from other rare human neuroendocrine tumors indicates that Merkel cell carcinoma, midgut carcinoid tumors, pheochromocytoma, and neuroblastoma tumor cells also express several of the main GPCR targets of imipramine and promethazine (Fig. 6A). Indeed, we found that both drugs are efficient in inducing rapid cell death in human cell lines from most of these cancer types as well as in mouse pancreatic neuroendocrine tumor cells, but not as strongly and efficiently as in non-neuroendocrine pancreatic adenocarcinoma cells (Supplementary Fig. S7B and Fig. 6B and C). We also tested neuroendocrine large cell carcinoma cells and large cell lung adenocarcinoma cells and found that they do not undergo significant cell death in response to both imipramine and promethazine (Supplementary Fig. S7B and Fig. 6B and C). We recently developed a novel model of pancreatic neuroendocrine tumors resulting from the deletion of *Rb*, *p53*, and *p130* in insulin-producing cells (*RIP-Cre Rb/p53/p130*, similar to the RIP-Tag model; ref. 43). These mice develop pancreatic tumors expressing insulin (Fig. 6D) and die approximately 2 months after birth (Fig. 6E). We found that treatment of these mice with imipramine starting at day 35 significantly increased survival (from 58 days for the mice injected with saline to 74.5 days for imipramine-treated mice; $P = 0.024$), further validating imipramine as a novel therapeutic agent against neuroendocrine tumors (Fig. 6E).

DISCUSSION

In this study, we used a systematic computational drug-repositioning strategy to identify FDA-approved TCAs and related molecules as potent inducers of cell death in SCLC cells through activation of stress pathways. We also show that the same drugs induce cell death in other types of neuroendocrine tumor cells. Together, these experiments elucidate a general mechanism of survival in neuroendocrine tumor cells and identify a common therapeutic strategy for a heterogeneous group of patients with cancer.

Our observations linking the survival of SCLC cells to the activity of GPCRs may be relevant to the biology of other tumors, including brain tumors, as suggested by epidemiologic studies (44), retinoblastoma (45), and pancreatic neuroendocrine tumors (46), which can be inhibited by drugs targeting neuronal signaling such as monoamine transmitters and receptors. Our study also illustrates the potential of drug-repositioning approaches, especially computational approaches, in the treatment of cancer. In this specific case, we were able to experimentally expand our findings in SCLC to other neuroendocrine tumors for which few gene expression profile datasets exist and for which the bioinformatics pipeline would not have been possible.

Our experiments suggest that inhibition of GPCRs at the surface of SCLC cells results in inhibition of PKA activity. An important aspect of future experiments will be to continue to investigate the signaling networks perturbed by these drugs in SCLC cells. We found that one important difference between SCLC and NSCLC cells is the rapid activation of the stress MAPK pathway in response to the candidate drugs. Thus, it will be interesting to determine if the engagement of different Gα subunits and downstream effectors explains the sensitivity of neuroendocrine cancer cells to these drugs. On a related note, we did not find a significant correlation between the mRNA expression levels of the candidate GPCRs and drug response in cancer cells. In particular, adenocarcinoma cells and other normal cells express these GPCRs at levels similar to SCLC cells, but do not die in response to the same drugs. It is probable that the total levels of these GPCRs on the surface of SCLC cells are not the determinant of the drug response but rather it is the activity of the molecular components of the signaling pathway downstream of the GPCRs and/or the activity of the ligands secreted by SCLC cells. Similar observations have been made recently in lung adenocarcinoma cells in which the effects of EGFR inhibition are not dependent on EGFR levels (47). Future experiments will be needed to shed light on the establishment of autocrine survival loops between

Published OnlineFirst September 26, 2013; DOI: 10.1158/2159-8290.CD-13-0183

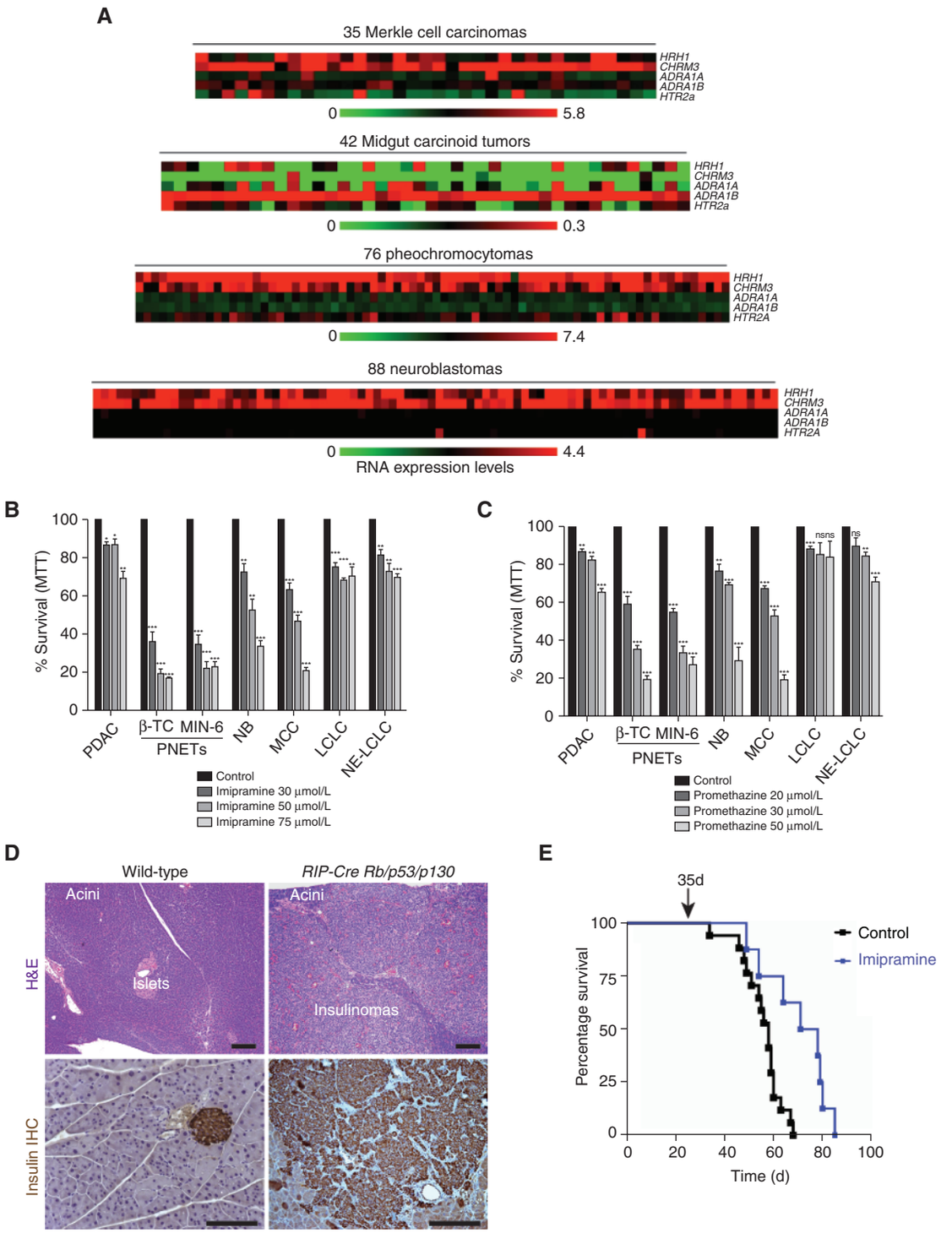

Figure 6. TCAs inhibit the growth of several other types of neuroendocrine tumors. **A,** heatmaps showing the normalized RNA expression levels of the H1R, CHRM3, ADRA1A, ADRA1B, and HTR2 in 35 human primary Merkel cell carcinomas, 42 midgut carcinoid tumors, 76 pheochromocytomas, and 88 neuroblastomas. **B** and **C,** MTT viability assays of human pancreatic adenocarcinoma (PDAC), mouse pancreatic neuroendocrine tumors (PNET), human neuroblastoma (NB), human Merkel cell carcinoma (MCC), human large cell adenocarcinoma (LCLC), and neuroendocrine large cell lung carcinoma (NE-LCLC) cultured in low serum and treated with increasing doses of imipramine (**B**) and promethazine (**C**) for 48 hours. Values from three independent experiments are shown as the mean ± SEM. *, $P < 0.05$; **, $P < 0.01$; ***, $P < 0.001$; ns, not significant. **D,** representative H&E images (top) and insulin immunohistochemistry (IHC; bottom) of sections from the pancreas of wild-type and *RIP-Cre Rb/p53/p130*–mutant mice. Scale bar is 50 μm. **E,** survival curve generated from the *RIP-Cre Rb/p53/p130* mice treated daily with intraperitoneal injections of saline and imipramine starting at day 35 after birth; median survival is 58 days for saline- and 74.5 days for imipramine-treated mutant mice; $P = 0.024$ by the Mantel–Cox test.

Published OnlineFirst September 26, 2013; DOI: 10.1158/2159-8290.CD-13-0183

GPCRs and their ligands in SCLC cells and to determine how these loops promote the survival of SCLC cells.

We have made a substantial effort to identify patients who may have been treated with TCAs incidentally as part of their routine care. Promethazine is sometimes used for nausea, but its heavily sedating effects limit its outpatient use to infrequent use. Much more commonly, the preferred phenothiazine antiemetic drug is prochlorperazine, as it is much less sedating. Even this drug is received only intermittently for the primary prevention of nausea from cisplatin and other chemotherapies. We have searched the electronic portion of the Stanford medical record (dating back to around the year 2000) for patients who received a TCA, and found fewer than five patients, none of whom were on the drugs chronically. Similarly, other database searches did not yield high patient numbers. On the basis of our preclinical results, prospective validation of these findings in a clinical trial setting has begun (NCT01719861—A phase IIa trial of desipramine in small cell lung cancer and other high-grade neuroendocrine tumors), but reportable results are not expected for years. An advantage of a drug-repositioning approach with approved medications for other indications is accelerated drug development times.

TCAs have largely been replaced in the clinic by a new generation of selective serotonin reuptake inhibitors. However, the anticancer effects of TCAs are in large part due to the less-specific, "off-target" mode of action of these drugs, which target multiple molecules at the surface of cells. The monoamine oxidase inhibitors tranylcypromine and pargyline do not antagonize these GPCRs and are not efficient in inducing cell death in SCLC cells. The fact that TCAs target multiple surface molecules has important consequences for patients with cancer: first, our analysis of gene expression profiles of SCLC and other neuroendocrine tumors indicates that most, if not all, individual tumors express at least one of these GPCRs. Thus, the vast majority of neuroendocrine tumors may be at least partly responsive to TCA treatment. In addition, acquired resistance to TCA treatment may take a long time to occur. Additional experiments in preclinical mouse models and early-phase clinical trials in patients with these FDA-approved drugs may help in rapidly identifying ways to translate these observations to better treatment options for patients with neuroendocrine tumors.

Finally, we believe that imipramine and other related TCAs could potentially be used as a second-line therapy in patients with SCLC who become refractory to cisplatin/etoposide. Our studies indicate that cisplatin-resistant tumors are still sensitive to imipramine treatment. We have tested the effects of combining imipramine with cisplatin at the early stages when the tumor was still sensitive to cisplatin *in vivo*, but we did not observe a significantly greater decrease in tumor growth compared with imipramine alone or cisplatin alone at the concentrations used; both drugs induce apoptotic cell death and may not induce more death together (data not shown). Moreover, the side-effect profile of TCAs is not benign, and combining with chemotherapy likely will substantially increase toxicity in a patient population with often compromised functional status, further reducing potential clinical benefit. On the basis of these observations, we propose that TCAs in the platinum refractory setting or as maintenance treatment after chemotherapy may be the most useful settings for these candidate drugs in clinical trials.

METHODS

Ethics Statement

Mice were maintained according to practices prescribed by the NIH (Bethesda, MD) at Stanford's Research Animal Facility, accredited by the Association for the Assessment and Accreditation of Laboratory Animal Care (AAALAC).

Drug-Repositioning and Bioinformatics Approach

The drug-repositioning analysis was based on a systematic approach described previously (4, 5). Detailed information can be found in the Supplementary Data.

Mice, Adenoviral Infections, and Subcutaneous Xenografts

The SCLC mouse model bearing deletions in *p53*, *Rb*, and *p130* (triple knockout) was previously described (15). The pancreatic neuroendocrine cancer mouse model is based on the deletion of *Rb*, *p53*, and *p130* in insulin-producing cells (*RIP-Cre Rb/p53/p130*, similar to the RIP-Tag model; ref. 43). This mouse model will be described in detail elsewhere. Ad-Cre (Baylor College of Medicine, Houston, TX) infections were carried out as previously described (14). Mice were maintained at the Stanford Research Animal Facility, accredited by the AAALAC. NSG mice were housed in the barrier facility at Stanford University (Stanford, CA). For the endogenous SCLC mice, treatment started 5 months after Ad-Cre infection. Imipramine (25 mg/kg), promethazine (25 mg/kg), and bepridil (10 mg/kg) were administered intraperitoneally daily for 30 consecutive days, whereas cisplatin (5 mg/kg) was administered intraperitoneally once weekly for a total of 6 to 8 weeks until tumors became chemoresistant. Chemonaïve tumors were generated after weekly injection of saline for a total of 6 weeks. Growth of these endogenous mouse tumors was monitored weekly by live imaging using Xenogen In Vivo Imaging System in the animal imaging facility at Stanford University, and quantification of the luciferase activity was calculated using the Living Image software. For subcutaneous injections, 0.5×10^6 mSCLC (Kp1, Kp3, saline-treated chemonaïve, and cisplatin-treated chemoresistant), and 2×10^6 hSCLC (H187 and H82) cells were injected into the two flanks of each NSG mouse with Matrigel (1:1; BD Biosciences). Treatment with the drugs started once the SCLC tumors reached 100 to 150 mm^3 (around 10–14 days after implantation). Imipramine (25 mg/kg), promethazine (25 mg/kg), and bepridil (10 mg/kg) were administered intraperitoneally daily for 36 to 48 consecutive days. Tumor volume was measured at the times indicated and calculated using the ellipsoid formula (length × $width^2$). The human primary SCLC sample was obtained from the National Disease Research Interchange program at the NIH. The tumor was digested with collagenase and dispase (Roche). Cells were collected and passed through a Magnetic-Activated Cell Sorting (Miltenyi Biotec) magnetic beads column to deplete $CD45^+$ blood cells. The remaining cells were injected into the flank of NSG mice with Matrigel (1:1) for expansion. Single-cell suspensions (1×10^6 and 3×10^6) from this new primary cell line (NJH29) were used for the primary human xenograft studies. Treatment with the drugs started once the xenografts reached 100 to 150 mm^3. Saline, imipramine (25 mg/kg), and promethazine (25 mg/kg) were administered intraperitoneally daily for 24 consecutive days.

Drugs and Inhibitors

Imipramine, promethazine, clomipramine, bepridil, necrostatin-1, azelastine, epinephrine, acetylcholine, serotonin, the histamine analog 2-(2-pyridyl) ethylamine, forskolin, and IBMX were all purchased from Sigma-Aldrich. Z-VAD-FMK, ritanserin, 4-DAMP, doxazosin mesylate, H89 dihydrochloride, KH7, and GF109203X were all purchased from Tocris Bioscience. The JNK inhibitor SP600125 was purchased from LC Laboratories. Fluo-3AM was purchased from Invitrogen. All these powders were dissolved in the appropriate solvent according to the manufacturer's instructions.

Cell Lines and Tissue Culture

Mouse SCLC cells (Kp1, Kp2, and Kp3) were grown in RPMI-1640 media containing 10% bovine growth serum (Fisher Scientific; ref. 15) or dialyzed FBS (dFBS; Fisher Scientific). NCI-H82, NCI-H69, and NCI-H187 human SCLC cells were obtained from American Type Culture Collection (ATCC) and cultured in RPMI media containing 10% serum. For the original cellular assays, we used the H82 cells because they grow very rapidly and enough cells can be obtained to conduct most of these assays. However, because they are the least sensitive of all three human SCLC cell lines, we used the other cell lines in the subsequent mechanistic experiments to investigate the mechanism of action of the drugs. The NSCLC cell lines A549 and LKR13 were a generous gift from Dr. A. Sweet-Cordero's laboratory (Stanford University). The NE-LCLC cell line H1155 was a generous gift from Dr. J. Minna's laboratory (UT Southwestern). Human pancreatic adenocarcinoma cell line PANC1, human neuroblastoma cell line HTB1, and LCLC NCI-1915 were obtained from ATCC and cultured in the same conditions described above. The Merkel cell carcinoma cell line was a generous gift from Dr. P. Nghiem's laboratory (University of Washington). The neuroendocrine mouse pancreatic cancer cells (MIN-6 and β-TC, both insulinomas) were a generous gift from Dr. S. Kim's laboratory (Stanford University) and were cultured in Dulbecco's Modified Eagle Medium containing high glucose (Thermo Scientific) and 15% serum. All mouse SCLC cell lines were generated in the Sage Laboratory and were authenticated by genotyping for the mutant alleles and the expression of neuroendocrine markers. All human cell lines were either repurchased from ATCC or given to us by other laboratories, except for NJH29, which was generated in the Sage Laboratory; no further authentication was carried out on these cell lines.

MTT Assays and Calcium Measurement

For MTT assays (Roche), floating cells were seeded at 8×10^4 (2% serum) or 1×10^5 (0.5% serum) per well in 96-well plates at day 0, and drugs were added on day 1. MTT reagents were added on day 2 or 3 depending on the experiments. The percentage survival was determined as the ratio of treated cells versus vehicle control. For all the rescue experiments, cells were pretreated with the various drugs or exogenous ligands for 30 minutes before the addition of imipramine or promethazine. Calcium measurements using the indicator Fluo-3AM were carried out per the manufacturer's instructions (Invitrogen). Briefly, trypsinized cells treated with the drugs in 2% serum at different time points were stained with 2.5 μmol/L Fluo-3AM for 30 minutes in RPMI media at 37°C. Cells were then washed in indicator-free RPMI media and then resuspended in PBS directly before being run through an Aria Analyzer fluorescence-activated cell sorting machine.

Immunoblot Analysis and Immunostaining

For immunoblotting, SCLC cells were homogenized using lysis buffer containing 1% NP-40, 50 mmol/L HEPES–KOH pH 7.8, 150 mmol/L NaCl, 10 mmol/L EDTA, and a cocktail of protease inhibitors. The antibodies used were phospho–stress-activated protein kinase (SAPK)/JNK Thr183 and Tyr185 (p-JNK), JNK, phospho-c-Jun Ser63 (p-c-Jun), c-Jun, phospho-CREB Ser133 (p-CREB antibody also recognizes p-ATF1), CREB, pan phospho-PKC βII Ser660 (p-PKC), PKC, and cleaved caspase-3 (all purchased from Cell Signaling technology), Karyopherin β1 (Santa Cruz Biotechnology), and α-tubulin (Sigma). We used 5-μm paraffin sections for H&E staining and immunostaining. Paraffin sections were dewaxed and rehydrated in the Trilogy reagent (Cell Marque). The primary antibodies used were phosphohistone 3 Ser10 (p-H3; Millipore), cleaved caspase-3 (CC3; Cell Signaling Technology), insulin (DAKO), and synaptophysin (SYN; Neuromics). Alexa Fluor secondary antibodies (Invitrogen) were used for antibody detection. Fluorescent images were captured on the Leica fluorescent microscope. For quantification of the number of CC3- and p-H3–positive cells, tumors of similar size and area ranging between 1,000 and 30,000 pixel units were included. Very small and very large tumors of areas measuring below or above this range were excluded.

Image Analysis and Statistics

Analysis of tumor areas and fluorescent images was conducted using ImageJ software by measuring pixel units. Mice were scored as having significant liver metastases if they had more than three metastases with at least 50 cells each. Statistical significance was assayed by a Student *t* test with the Prism GraphPad software (two-tailed unpaired and paired *t* test depending on the experiment). *, $P < 0.05$; **, $P < 0.01$; ***, $P < 0.005$; ns, not significant. Data are represented as the mean ± SEM. For the survival curve analysis and comparison, we used the Mantel–Cox test.

Disclosure of Potential Conflicts of Interest

Patents have been filed and are pending on the use of specific tricyclic antidepressants in neuroendocrine tumors. A.J. Butte, J.T. Dudley, J. Sage, and N.S. Jahchan are inventors on the patent, and could benefit with royalties. The intellectual property has been licensed to NuMedii, a company further developing these drugs. A.J. Butte and J.T. Dudley are founders and shareholders in NuMedii.

Authors' Contributions

Conception and design: N.S. Jahchan, J.T. Dudley, A.J. Butte, J. Sage
Development of methodology: N.S. Jahchan, J.T. Dudley, K. Krasinska, A.J. Butte
Acquisition of data (provided animals, acquired and managed patients, provided facilities, etc.): N.S. Jahchan, P.K. Mazur, N. Flores, D. Yang, A. Palmerton, A.-F. Zmoos, K.Q.T. Tran, M. Zhou, K. Krasinska, K.S. Park
Analysis and interpretation of data (e.g., statistical analysis, biostatistics, computational analysis): N.S. Jahchan, J.T. Dudley, P.K. Mazur, N. Flores, D. Yang, A. Palmerton, D. Vaka, K.Q.T. Tran, M. Zhou, K. Krasinska, J.W. Neal, P. Khatri, A.J. Butte, J. Sage
Writing, review, and/or revision of the manuscript: N.S. Jahchan, J.T. Dudley, A. Palmerton, J.W. Riess, J.W. Neal, A.J. Butte, J. Sage
Study supervision: A.J. Butte, J. Sage

Acknowledgments

The authors thank Dr. Anton Berns for the *Trp53*^{lox} mice, Dr. Luis Parada for helpful comments, the Sweet-Cordero Laboratory for suggestions throughout the project, cell lines, and antibodies, Dr. Brian Kobilka and Dr. Pawel Niewiadomski for helpful discussions on GPCR signaling, Andrew Kruse for conducting the binding assay to measure the number of mAchR, Dr. Paul Nghiem for the MCC cell line, Dr. Seung Kim for the pancreatic neuroendocrine cell lines, Alex Augustyn and Dr. John Minna for the neuroendocrine large cell lung cancer cell lines, and members of the Sage Laboratory for their help throughout the course of this study.

Grant Support

This work was supported by the Lucile Packard Foundation for Children's Health (to J. Sage), the Department of the Army (W81XWH-13-1-0211; to J. Sage), the National Library of Medicine (NLM) Biomedical Informatics Training Grant (T15 LM007033) to Stanford University (to J.T. Dudley), the National Institute of General Medical Sciences (NIGMS) R01 GM079719 (to A.J. Butte), the National Cancer Institute (5R01CA138256-04; to A.J. Butte and J. Sage), the Stanford Dean's Fellowship, NRSA T32 Academic Research Training in Pulmonary Medicine, and a California Tobacco Related Disease Research Program (TRDRP) postdoctoral fellowship (to N.S. Jahchan), and a Stanford Cancer Institute Developmental Cancer Research award (to J.W. Neal and J.W. Riess).

Received April 23, 2013; revised August 20, 2013; accepted August 22, 2013; published OnlineFirst September 27, 2013.

Published OnlineFirst September 26, 2013; DOI: 10.1158/2159-8290.CD-13-0183

REFERENCES

1. Ashburn TT, Thor KB. Drug repositioning: identifying and developing new uses for existing drugs. Nat Rev Drug Discov 2004;3:673–83.
2. Li YY, An J, Jones SJ. A computational approach to finding novel targets for existing drugs. PLoS Comput Biol 2011;7:e1002139.
3. Yang L, Agarwal P. Systematic drug repositioning based on clinical side-effects. PLoS ONE 2011;6:e28025.
4. Dudley JT, Sirota M, Shenoy M, Pai RK, Roedder S, Chiang AP, et al. Computational repositioning of the anticonvulsant topiramate for inflammatory bowel disease. Sci Transl Med 2011;3:96ra76.
5. Sirota M, Dudley JT, Kim J, Chiang AP, Morgan AA, Sweet-Cordero A, et al. Discovery and preclinical validation of drug indications using compendia of public gene expression data. Sci Transl Med 2011;3:96ra77.
6. Cheng F, Liu C, Jiang J, Lu W, Li W, Liu G, et al. Prediction of drug–target interactions and drug repositioning via network-based inference. PLoS Comput Biol 2012;8:e1002503.
7. van Meerbeeck JP, Fennell DA, De Ruysscher DK. Small-cell lung cancer. Lancet 2011;378:1741–55.
8. Heist RS, Engelman JA. SnapShot: non–small cell lung cancer. Cancer Cell 2012;21:448 e2.
9. Neal JW, Gubens MA, Wakelee HA. Current management of small cell lung cancer. Clin Chest Med 2011;32:853–63.
10. Byers LA, Wang J, Nilsson MB, Fujimoto J, Saintigny P, Yordy J, et al. Proteomic profiling identifies dysregulated pathways in small cell lung cancer and novel therapeutic targets including PARP1. Cancer Discov 2012;2:798–811.
11. Wistuba II, Gazdar AF, Minna JD. Molecular genetics of small cell lung carcinoma. Semin Oncol 2001;28:3–13.
12. Moody TW, Chan D, Fahrenkrug J, Jensen RT. Neuropeptides as autocrine growth factors in cancer cells. Curr Pharm Des 2003;9:495–509.
13. Onganer PU, Seckl MJ, Djamgoz MB. Neuronal characteristics of small-cell lung cancer. Br J Cancer 2005;93:1197–201.
14. Park KS, Martelotto LG, Peifer M, Sos ML, Karnezis AN, Mahjoub MR, et al. A crucial requirement for Hedgehog signaling in small cell lung cancer. Nat Med 2011;17:1504–8.
15. Schaffer BE, Park KS, Yiu G, Conklin JF, Lin C, Burkhart DL, et al. Loss of p130 accelerates tumor development in a mouse model for human small-cell lung carcinoma. Cancer Res 2010;70:3877–83.
16. Kiselyov K, Shin DM, Muallem S. Signalling specificity in GPCR-dependent Ca^{2+} signalling. Cell Signal 2003;15:243–53.
17. Thompson MD, Burnham WM, Cole DE. The G protein–coupled receptors: pharmacogenetics and disease. Crit Rev Clin Lab Sci 2005;42:311–92.
18. Berridge MJ, Lipp P, Bootman MD. The versatility and universality of calcium signalling. Nat Rev Mol Cell Biol 2000;1:11–21.
19. Perry PJ, Zeilmann C, Arndt S. Tricyclic antidepressant concentrations in plasma: an estimate of their sensitivity and specificity as a predictor of response. J Clin Psychopharmacol 1994;14:230–40.
20. Fisar Z, Krulik R, Fuksova K, Sikora J. Imipramine distribution among red blood cells, plasma and brain tissue. Gen Physiol Biophys 1996;15:51–64.
21. Petersen RC, Richelson E. Anticholinergic activity of imipramine and some analogs at muscarinic receptors of cultured mouse neuroblastoma cells. Psychopharmacology 1982;76:26–8.
22. Chen G, Hasanat KA, Bebchuk JM, Moore GJ, Glitz D, Manji HK. Regulation of signal transduction pathways and gene expression by mood stabilizers and antidepressants. Psychosom Med 1999;61:599–617.
23. Assanasen P, Naclerio RM. Antiallergic anti-inflammatory effects of H1-antihistamines in humans. Clin Allergy Immunol 2002;17:101–39.
24. Donati RJ, Rasenick MM. G protein signaling and the molecular basis of antidepressant action. Life Sci 2003;73:1–17.
25. Lopez-Munoz F, Alamo C. Monoaminergic neurotransmission: the history of the discovery of antidepressants from 1950s until today. Curr Pharm Des 2009;15:1563–86.
26. Fribourg M, Moreno JL, Holloway T, Provasi D, Baki L, Mahajan R, et al. Decoding the signaling of a GPCR heteromeric complex reveals a unifying mechanism of action of antipsychotic drugs. Cell 2011;147:1011–23.
27. Bhattacharjee A, Richards WG, Staunton J, Li C, Monti S, Vasa P, et al. Classification of human lung carcinomas by mRNA expression profiling reveals distinct adenocarcinoma subclasses. Proc Natl Acad Sci U S A 2001;98:13790–5.
28. Rohrbeck A, Neukirchen J, Rosskopf M, Pardillos GG, Geddert H, Schwalen A, et al. Gene expression profiling for molecular distinction and characterization of laser captured primary lung cancers. J Transl Med 2008;6:69.
29. Greshock J, Bachman KE, Degenhardt YY, Jing J, Wen YH, Eastman S, et al. Molecular target class is predictive of in vitro response profile. Cancer Res 2010;70:3677–86.
30. Heasley LE. Autocrine and paracrine signaling through neuropeptide receptors in human cancer. Oncogene 2001;20:1563–9.
31. Song P, Sekhon HS, Lu A, Arredondo J, Sauer D, Gravett C, et al. M3 muscarinic receptor antagonists inhibit small cell lung carcinoma growth and mitogen-activated protein kinase phosphorylation induced by acetylcholine secretion. Cancer Res 2007;67:3936–44.
32. Zhang S, Togo S, Minakata K, Gu T, Ohashi R, Tajima K, et al. Distinct roles of cholinergic receptors in small cell lung cancer cells. Anticancer Res 2010;30:97–106.
33. Rasenick MM, Chaney KA, Chen J. G protein–mediated signal transduction as a target of antidepressant and antibipolar drug action: evidence from model systems. J Clin Psychiatry 1996;57(Suppl 13):49–55.
34. Hill SJ. Distribution, properties, and functional characteristics of three classes of histamine receptor. Pharmacol Rev 1990;42:45–83.
35. Billington CK, Penn RB. m3 muscarinic acetylcholine receptor regulation in the airway. Am J Respir Cell Mol Biol 2002;26:269–72.
36. Chen ZJ, Minneman KP. Recent progress in alpha1-adrenergic receptor research. Acta Pharmacol Sin 2005;26:1281–7.
37. Traish AM, Moreland RB, Gallant C, Huang YH, Goldstein I. G-protein–coupled receptor agonists augment adenylyl cyclase activity induced by forskolin in human corpus cavernosum smooth muscle cells. Recept Signal Transduct 1997;7:121–32.
38. Lonze BE, Ginty DD. Function and regulation of CREB family transcription factors in the nervous system. Neuron 2002;35:605–23.
39. Shinoura H, Shibata K, Hirasawa A, Tanoue A, Hashimoto K, Tsujimoto G. Key amino acids for differential coupling of alpha1-adrenergic receptor subtypes to Gs. Biochem Biophys Res Commun 2002;299:142–7.
40. Moniri NH, Booth RG. Role of PKA and PKC in histamine H1 receptor-mediated activation of catecholamine neurotransmitter synthesis. Neurosci Lett 2006;407:249–53.
41. Schroder R, Janssen N, Schmidt J, Kebig A, Merten N, Hennen S, et al. Deconvolution of complex G protein-coupled receptor signaling in live cells using dynamic mass redistribution measurements. Nat Biotechnol 2010;28:943–9.
42. Gerits N, Kostenko S, Shiryaev A, Johannessen M, Moens U. Relations between the mitogen-activated protein kinase and the cAMP-dependent protein kinase pathways: comradeship and hostility. Cell Signal 2008;20:1592–607.
43. Hanahan D. Heritable formation of pancreatic beta-cell tumours in transgenic mice expressing recombinant insulin/simian virus 40 oncogenes. Nature 1985;315:115–22.
44. Walker AJ, Card T, Bates TE, Muir K. Tricyclic antidepressants and the incidence of certain cancers: a study using the GPRD. Br J Cancer 2011;104:193–7.
45. McEvoy J, Flores-Otero J, Zhang J, Nemeth K, Brennan R, Bradley C, et al. Coexpression of normally incompatible developmental pathways in retinoblastoma genesis. Cancer Cell 2011;20:260–75.
46. Li L, Hanahan D. Hijacking the neuronal NMDAR signaling circuit to promote tumor growth and invasion. Cell 2013;153:86–100.
47. Lee MJ, Ye AS, Gardino AK, Heijink AM, Sorger PK, MacBeath G, et al. Sequential application of anticancer drugs enhances cell death by rewiring apoptotic signaling networks. Cell 2012;149:780–94.